Downloaded from orbit.dtu.dk on: May 05, 2023

DTU Library

Physics Department. Annual progress report 1 January - 31 December 1973

Research Establishment Risø, Roskilde

Publication date:
1973

Document Version
Publisher's PDF, also known as Version of record

Link back to DTU Orbit

Citation (APA):
Research Establishment Risø, R. (1973). *Physics Department. Annual progress report 1 January - 31 December 1973*. Risø National Laboratory. Denmark. Forskningscenter Risoe. Risoe-R No. 300

General rights
Copyright and moral rights for the publications made accessible in the public portal are retained by the authors and/or other copyright owners and it is a condition of accessing publications that users recognise and abide by the legal requirements associated with these rights.

- Users may download and print one copy of any publication from the public portal for the purpose of private study or research.
- You may not further distribute the material or use it for any profit-making activity or commercial gain
- You may freely distribute the URL identifying the publication in the public portal

If you believe that this document breaches copyright please contact us providing details, and we will remove access to the work immediately and investigate your claim.

[redacted]

Risø Report No. 300

Danish Atomic Energy Commission

Research Establishment Risø

Physics Department
Annual Progress Report

1 Januar – 31 December 1973

December 1973

Sales distributors: Jul. Gjellerup, 87, Sølvgade, DK-1307 Copenhagen K, Denmark
Available on exchange from: Library, Danish Atomic Energy Commission, Risø, DK-4000 Roskilde, Denmark

UDC 53

December 1973

Risø Report No. 300

Danish Atomic Energy Commission
Research Establishment Risø

PHYSICS DEPARTMENT ANNUAL PROGRESS REPORT

1 January - 31 December 1973

edited by
H. Bjerrum Møller and B. Lebech

This report contains unpublished results and should not be quoted without permission from the authors.

ISBN 87 550 0242 0

CONTENTS

SUMMARY

The research work in the Physics Department at Risø covers four main fields:

Solid-State Physics (Neutron Scattering)

Plasma Physics

Nuclear Spectroscopy

Meteorology

The principal activities in these fields are presented in this report covering the period from 1 January to 31 December 1973.

The solid-state physics section utilizes thermal neutron beams from the DR 3 reactor for experimental studies of solids and liquids. Six neutron spectrometers are available for these experiments: Three 3-axis, two 2-axis, and one multiangle-reflecting crystal spectrometer with a position-sensitive detector (MARX spectrometer). An additional diffractometer is used for structural studies by the Institute of Chemistry, University of Århus. The liquid-hydrogen cold source is nearly ready for installation in the DR 3 reactor. Cold neutrons will presumably be available from the spring of 1974. The construction of neutron-conducting tubes from the cold source to an experimental hall was continued, and they are planned to be installed in the spring of 1974.

The scientific investigations can be roughly classified as lying within the following fields: magnetism, lattice dynamics, liquids, and amorphous materials.

The crystal-field parameters of $LiTbF_4$ were determined, and they confirmed that $LiTbF_4$ can be considered as an Ising ferromagnet at low temperatures. A study of the critical scattering from this model system (dipolar Ising ferromagnet) was initiated.

The long-range order of β-brass was remeasured with proper attention to the important corrections arising from extinction in the crystal and the difference in scattering amplitude of the Cu and Zn.

Several magnetic compounds of the rutile structure were investigated by elastic neutron diffraction. No signs of superlattice reflections were observed presumably on account of the random arrangement of the magnetic ions.

The magnetic form factor of Fe was further examined by measurement of the intensity of critical scattering around the forward direction. The

form factor was found to be larger than unity for small wave vectors. In addition a central peak was observed in the energy spectrum and interpreted as longitudinal critical scattering.

Several experiments were performed on Pr: The form factor was measured and the corresponding radial wave function showed a 12% expansion compared to non-relativistic calculations. The magnetic exitons were further investigated using a larger crystal. Particular attention was paid to the mode of minimum energy along ΓM. The energy of this mode decreases as the temperature is reduced from 30 to 6.0 K. Experiments at lower temperatures are planned to investigate if this mode goes soft at a possible ordering temperature of Pr. A theory for the dispersion relation and temperature variation of the lowest excited states in Pr has been developed.

The magnetic structure investigations of Nd in strong magnetic fields have been pursued and the results have been interpreted in terms of a model which includes the influence on the cubic sites of the ordering in the hexagonal sites.

Crystal-field parameters were determined in $PrFeO_3$ and in Nd-chalcogenides, and theories were developed for the Nd-group V compounds and for the rare earth-Al_2 compounds. The magnetic exciton dispersion relation in $NdAl_2$ was measured and compared with the theory. In $TbAl_2$ a magnon to magnetic exciton interaction was observed. As the temperature is raised, the renormalized magnon energy approaches and crosses the energy difference between the two high-lying single ion states. This gives rise to a magnon-exciton coupling which appears as two mixed modes in the experiment.

The effect on the spin wave spectrum of diluting the magnetic insulator CoF_2 with Zn was investigated and is being analysed at present.

Specific heat and NMR data on EuO and EuS was reanalysed and shown to be consistent with the exchange constant determined by neutron scattering.

Spin waves and sublattice magnetization of the near-Heisenberg, planar antiferromagnet $NiCl_2$ have been measured and compared with a renormalized spin wave theory.

Previously, the single-ion anisotropy and the anisotropy of the exchange interaction have been studied by measurements of the spin wave energies of Tb in applied magnetic fields. These measurements have now been corrected for the field dependence of the relative magnetization and, in the case of the anisotropic exchange, for the influence of the magnon-phonon interaction. These corrections modify the results to some extent. The

exchange interaction is very anisotropic at low temperatures, but above 150 K the interaction is essentially isotropic.

The dispersion relation for spin waves in the conical magnetic phase of Er measured at Oak Ridge has been reanalysed using an alternative kind of anisotropic coupling between the total angular moments. The resulting anisotropy is reduced by an order of magnitude.

An intuitively simple and computationally fast approach to electronic energy bands and wave functions has been applied to Yb, with the aim of examining a possible origin of the hcp to fcc phase transition under pressure. It is hoped that this approach will also make possible theoretical calculations of crystal fields, exchange interactions, and the electronic structures of more complicated materials.

A number of theoretical investigations relating to the magnetism of the heavy rare-earth metals were carried out: The exchange interaction was calculated from the energy bands for Gd, Tb, Dy and Er. The temperature dependence of the ferromagnetic resonance energy was expressed as a function of correlation functions of tensor operators in the Hamiltonian. The temperature dependence of the macroscopic single-ion anisotropy constants was investigated in the spin wave theory. It was shown that the product of two angular momentum operators can generally be expressed in a series of single tensor operators, and a hermitian Bose expansion of tensor operators of arbitrary rank was derived.

An inelastic neutron scattering investigation of Ta was initiated, with the aim of investigating anomalies of the phonon dispersion relations (energy shifts and widths) associated with the superconducting phase.

A neutron scattering study of deuterated CsDA at temperatures around the ferroelectric transition was carried out. No signs of critical scattering were observed, but sets of non-commensurate side peaks to the Bragg reflections were observed above the transition temperature, indicating a periodic structure.

Measurements of the (free) rotational mode in the plastic crystal C_2F_6 have been initiated.

An investigation of the nematic to isotropic phase transition in the liquid crystal PAA showed critical scattering around two temperatures which are interpreted as the stability limits of the isotropic and nematic phase respectively.

The neutron diffraction study of amorphous ice was completed. The static structure factor $S(\underline{\kappa})$ was obtained from the data, and by a Fourier transformation the radial distribution function was derived.

The static structure factor of amorphous Se determined from neutron diffraction showed several distinct peaks. A search for excitations in amorphous Se is planned.

Preliminary neutron scattering experiments in liquid N_2 showed signs of the existence of a sound wave in a wave vector region where hydrodynamic theory yields an overdamped mode. Indications of a coupling between rotational and translational modes were also observed.

A number of new experimental techniques were investigated. Apparatus for neutron scattering from samples at a hydrostatic pressure up to 2 kbars was finished, and measurements of the pressure and temperature dependence of the structure and dynamics of solid D_2 and H_2 have been started. Apparatus for measurement on powdered samples or single crystals in a fixed scattering geometry at pressures up to 35 kbars was further developed and is presently used in investigations of Cr. Further investigations of the neutron slowing-down by Bragg reflection from a moving single crystal were carried out.

The plasma physics section works primarily in two fields: technology of interest for future fusion reactors (utilizing a puffatron and a magnetically driven shock tube) and basic plasma properties (utilizing a Q-machine).

The interaction between a plasma and a solid is very complex. A further experiment to study the bombardment of a solid target by particles in the keV range was prepared and constructed. The target layer is made by letting e.g. H_2 solidify on a cold quartz crystal. This technique was tested and the first irradiation of the target will take place soon.

The puffatron produces a hot rotating plasma in a strong radial electric and axial magnetic field. Studies of the interaction between the plasma and solids injected into the plasma were pursued both experimentally and theoretically, with a possible refuelling scheme for future fusion reactors in mind. A launcher of solid H_2 pellets operates on the puffatron, so that a pellet can be shot into the plasma region. Measurements of the dependence of the pellet mass loss on plasma energy for H and He plasmas showed higher losses than expected theoretically. A preliminary determination of the ion energy spectrum by means of a neutral particle detector indicates that high-energy neutrals are detected for a longer period when a pellet is present. Part of these investigations were a continuation of the collaboration with Culham (UKAEA, England).

In the shock tube a strong shock moving at a constant speed is produced electromagnetically through the interaction between a constant driving current and its self-magnetic field. A theoretical and experimental study of the distance between the shock and the current sheet was made and work to determine the refractivity of the plasma was initiated.

The Q-machine produces a relatively cold dc-plasma (2000 K) from ionized Cs. As a possible means of increasing the electron temperature range, electron heating by microwaves at the cyclotron resonance frequency was examined.

After the magnetic field was modified into a cusp field the frequency spectrum of the ion acoustic turbulence was measured. The Farley instability was investigated in a case where a radial electric field was applied to the plasma. A thorough theoretical study of ion wave propagation in stable and unstable plasmas gives the basic for future experimental work.

The nuclear physics section works on problems related to fission. An experiment to study fission isomers resulting from the absorption of neutron in ^{235}U has been built at the DR 3 reactor. Preliminary measurements indicate that ratios of isomer to prompt fission of 10^{-5} can be observed in the experiment.

The meteorology section is primarily engaged in studies of the planetary boundary layer. The efforts can be roughly classified as follows: (1) Micrometeorological research, (2) Climatological investigations, (3) Development of meteorological instruments, and (4) Applied meteorology.

The micrometeorological research aims at descriptions of the structure of atmospheric turbulence and its dependence on external parameters such as surface characteristics and the synoptic weather situation. An important goal is parameterization of the transport properties of atmospheric turbulence, so that the planetary boundary layer can be realistically incorporated in numerical weather prediction schemes.

Air - sea interaction is a problem to which the section pays increasing attention. The interest is primarily concentrated on turbulence and fluxes in the lowest 20 m above the sea. In co-operation with oceanographers from the University of Copenhagen and the University of Bergen, an instrumented tower was erected on 25 m of water in the Kattegat. The meteorology section also participated in the Second Joint North Sea Wave Project. Both projects were subject to a series of mishaps beyond the section's control. However, valuable data and experience were gained in the experments.

At Risø a 120 m tower is available for experimental work. Meteorological parameters such as wind speed and directions, temperatures and humidities are measured routinely at a number of heights. As a result of the measurements, data records are available containing 15 years of hourly readings. The records are used extensively by the section and by others.

For field experiments the section has at its disposal a 50 m mobile tower and a data acquisition system installed in a van. The digital data system is capable of sampling 60 signals simultaneously at a rate of 200 times per second.

In collaboration with the Danish Meteorological Institute, two unmanned climatological observatories were designed and brought into operation in Northeastern Greenland. The analysis of climatological data from Greenland, Risø, and other locations in Denmark was continued. Special emphasis is given to analyses in terms of spectral characteristics of weather and climate fluctuations. Extreme-value statistics is being applied to wind data with special regard to wind loading of buildings and other structures. An attempt is made to construct a numerical model which can demonstrate the effect of diurnal changes in the wind structure of the planetary boundary layer.

This year as earlier, the meteorology section undertook a number of tasks of an applied nature. Among them were: Site evaluation for nuclear power stations and dispersion modelling, development and testing of meteorological instruments, air pollution studies, and evaluation of dynamic effects of wind on engineering structures.

1. SOLID-STATE PHYSICS (NEUTRON SCATTERING)

$LiTbF_4$ - A Dipolar Ising Ferromagnet

(J. Als-Nielsen and L. M. Holmes[x])

Holmes et al. recently discovered from their bulk susceptibility data[1] that the dominant interaction between the magnetic moments of the Tb ions in $LiTbF_4$ might well be the dipolar interaction. They also found that the excited levels of the Tb ions were about 200 K above the ground state level. A more detailed investigation of the crystal field levels was carried out by inelastic neutron scattering techniques. Spectra at different temperatures and with the wave vector along two symmetry directions giving different selection rules for the transitions are shown in fig. 1. The data were analysed in terms of the crystal field Hamiltonian

$$H_c = \sum_{kqi} B_{kq}(C_q^{(k)})_i \qquad (1)$$

with $C_q^{(k)}$ being proportional to spherical harmonics Y_k^q and the summation i being over the Tb^{3+} electrons.

The number of terms which need to be included depends on J and on the site symmetry. For J = 6 in symmetry S_4, the number of terms may be reduced, leaving six independent crystal field parameters B_{kq} to be determined. The parameters derived for $LiTbF_4$ are $B_{20} = 316$, $B_{40} = -673$, $B_{44} = 628$, $B_{60} = -338$, Re $B_{64} = 82$, and Im $B_{64} = -92\ cm^{-1}$. The fit to the experimental data is also illustrated in fig. 1, where the curves have been scaled to the magnetic quasi-elastic peak at low temperatures. The dashed line shows the assumed background for all the curves. The intensities were not used as inputs in the fitting procedure, and the agreement between theory and experiment is quite reasonable in view of the complexity of the problem. With these crystal field parameters the measured susceptibility fits the theory perfectly, which is a distinct improvement over the rough theoretical approximations used in [1].

[x] Present address: ETH, Zürich, Switzerland

1) L. M. Holmes, T. Johansson, and H. J. Guggenheim, Solid State Commun. 12, 993 (1973)

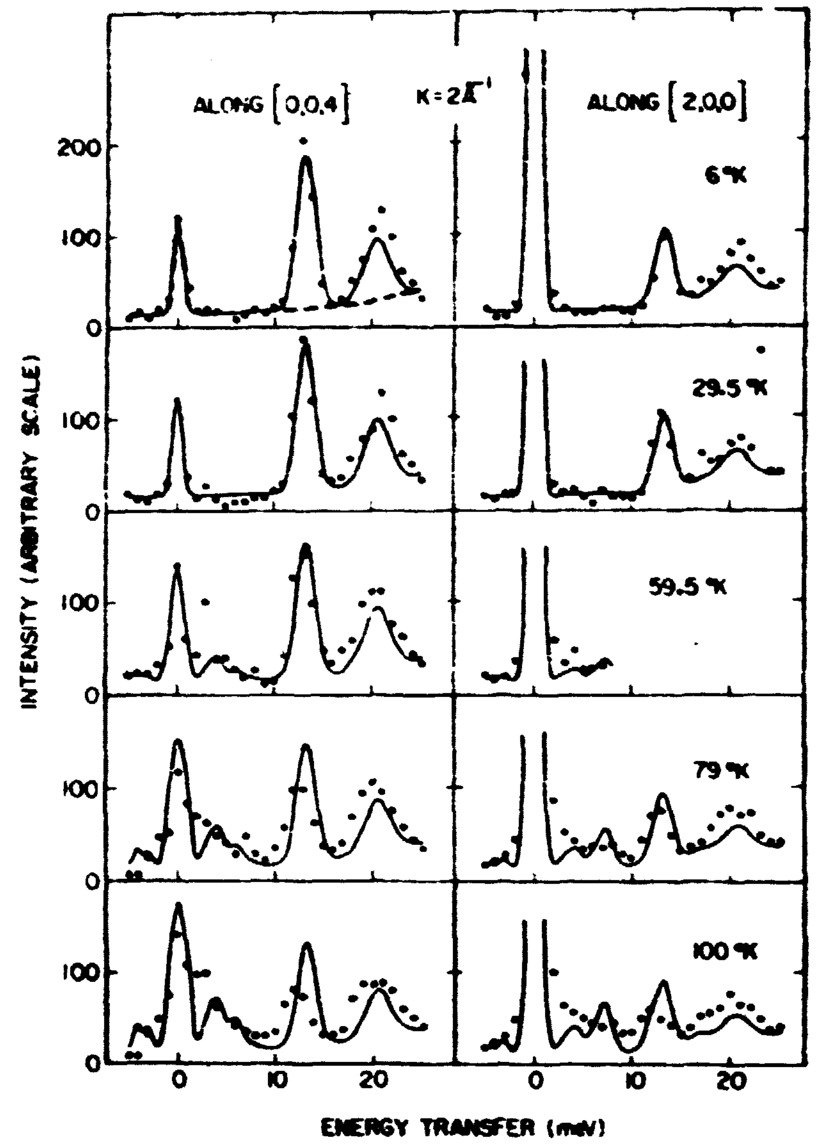

Fig. 1. Inelastic neutron spectra in $LiTbF_4$. The scans were taken with a fixed, filtered analyser energy of 14.3 meV using collimations of 36, 62, 47, 62 min of arc. Solid curves are theoretical, normalized to the quasi-elastic intensity for κ along [2, 0, 0]. Dashed line shows assumed background correction for all curves.

We shall now consider the ferromagnetic ordering at $T_c = 2.865$ K in more detail. The elastic magnetic scattering around (2, 0, 0) is proportional to the longitudinal wave vector dependent susceptibility $\chi(\underline{q}, T)$. At high temperatures $\chi(\underline{q}, T)$ is given by the Curie-Weiss relation generalised to the wave vector dependent susceptibility, $\chi(q, T) = T/(T - \theta(\underline{q}))$. The Curie-Weiss temperature $\theta(q)$ is essentially the Fourier transform of the interaction between the magnetic moments. For dipolar Coulomb interactions $\theta(\underline{q})$ contains the well-known $q = 0$ singularity. For small q, $\theta(\underline{q})$ is given by

$$\theta(\underline{q}) = \theta_x\{1 - (1+\theta_z/\theta_x)(q_z/q)^2 - \rho_x^2 q^2 + (\rho_x^2 + \rho_z^2)q_z^2\} . \qquad (2)$$

It is seen that $\theta(\underline{q})$ goes to $+\theta_x$ when $\underline{q}$ is approaching 0 along the x-axis, but $\theta(q)$ goes to $-\theta_z$ when $\underline{q}$ is approaching 0 along the z-axis, i.e. along the spin direction. The values of the quantities in (2) have been determined numerically as $\theta_x = 3.925$ K, $\theta_z = 4.48$ K, $\rho_x = 1.06$ Å^2, $\rho_z = 1.37$ Å^2. The value of θ_x may be compared with the Curie-Weiss temperature of 3.65 K obtained in [1] by fitting bulk susceptibility data to (2) in the region 15 K < T < 30 K. From elastic neutron scattering data in the same temperature region we have found that the four parameters θ_x, θ_z, ρ_x, and ρ_z are all close to the values calculated for dipolar interactions. These results thus strongly support the statement that $LiTbF_4$ may be regarded as an Ising magnet with the moments coupled exclusively by dipolar interactions. The crystal field study shows that the excited states can be neglected for temperatures at least up to 20 T_c. It is therefore of considerable interest to study the critical phenomena in this model system, especially in the light of the recent theoretical development in critical phenomena known as the Wilson-Fisher renormalization group theory. We have initiated a study of the critical neutron scattering. Results will be published during 1974.

Long-Range Order in β-Brass

(O. Rathmann and J. Als-Nielsen)

β-Brass is an alloy of almost equal amounts of Cu and Zn. At room temperature it has an almost perfectly ordered CsCl structure with Cu atoms occupying the cube corners (the A-sublattice) and Zn atoms occupying the cube centres (the B-sublattice). As the temperature is increased, the occupation of lattice sites becomes more and more random until at the critical temperature T_c there are just as many Cu atoms as Zn atoms in each sublattice. The average occupation of a sublattice is called the long-range order, M(T). It can be determined by the intensity of a superlattice Bragg reflection in a diffraction experiment. Neglecting thermal vibrations for a moment, the scattering powers of the A and B sublattices are $f_{Cu} \cdot M(T)$ and $f_{Zn} \cdot M(T)$ respectively, and as the wave scattered from the A sublattice is out of phase with the wave scattered from the B sublattice, the resulting intensity is proportional to $(f_{Cu} - f_{Zn})^2 \cdot M^2(T)$.

In the past there have been numerous attempts to determine M(T) from diffraction experiments, both by X-ray diffraction and neutron diffraction. The motivation for these efforts is the formal similarity between the order - disorder transition in the AB alloy and the transition from the ferromagnetic to the paramagnetic phase in the Ising model.

Unfortunately the latest X-ray results[2] did not agree with the earlier neutron scattering results[3]. The present study was initiated in order to find the reason for the discrepancy and to determine the long-range order in β-brass once and for all. There are two important effects to be considered. First of all the thermal vibrations of the lattice cannot be neglected, and furthermore the A and B sublattices do not vibrate in the same way. In the ordered phase, the Cu sublattice vibrates much more than the Zn sublattice and this effect is particularly important in X-ray diffraction because the scattering powers of Cu and Zn are almost equal. Secondly, it must be ensured that the diffracting lattice planes are uniformly illuminated at all temperatures, i. e. that extinction can be neglected, or accurately corrected for. Here X-ray diffraction is more practical than neutron diffraction because the scattering power of superlattice Bragg scattering is of the same order of magnitude in the two cases. For X-rays the effective sample thickness is automatically small ($\sim$0.02 mm). owing to the photo-absorption, whereas a suitable thin crystal must be prepared for the neutron scattering experiments. In contrast to the previous neutron experiment our sample was now thin enough to reduce the extinction to about 1 %. Thus, in the present study both effects distorting the data from the simple $M^2(T)$ dependence were small.

Our present results, fig. 2, are in excellent agreement with the X-ray results, although the raw data of the two methods are quite different. The experimental results deviate significantly from the Ising model prediction. However, the critical exponent, β, describing M(T) near T_c, $M(T) = D(1-T/T_c)^{\beta}$, is in agreement with the Ising model prediction, of $\beta = 0.30$. The discrepancy is only in the amplitude D, where the experimental value is $D = 1.64$, whereas the Ising model value is $D = 1.50$.

2) D. R. Chipman and C. B. Walker, Phys. Rev. B5, 3823 (1972)

3) J. C. Norvell and J. Als-Nielsen, Phys. Rev. B2, 277 (1970)

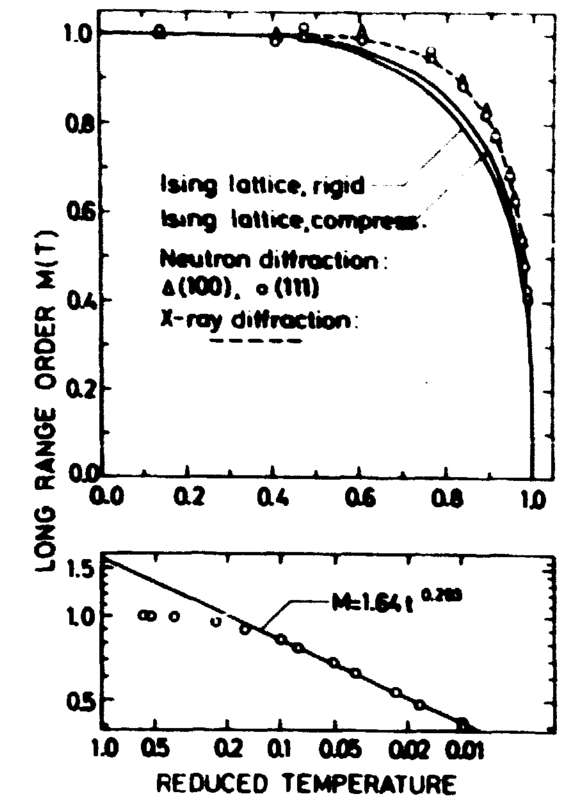

Fig. 2. The long range order in β-Brass as determined in the present neutron experiment from the (100) and (111) superlattice reflections. The data were normalized to 1 at 300 K. Also shown in the upper part of the figure is the result of the X-ray experiment by Chipman and Walker[2] and the predictions of the rigid and the compressible Ising lattice model (upper and lower solid lines respectively).
In the lower part of the figure the (100) neutron data are shown in a log-log-plot, displaying the asymptotic behaviour.

Magnetic Ordering Properties of $CrNbO_4$, $FeNbO_4$, and $FeTaO_4$

(A. Nørlund Christensen (University of Århus), T. Johansson (Technical University of Denmark), and B. Lebech)

The compounds $CrNbO_4$, $FeNbO_4$, and $FeTaO_4$ can have crystal structures of the rutile type in which the metal ions may be arranged at random. An investigation of the magnetic properties of the compounds was initiated. Magnetization measurements from 4.2 to 300 K show a minimum in the inverse susceptibility, $1/\chi$, at 9.3 K for $CrNbO_4$ and at 46 K for $FeNbO_4$.

For $CrNbO_4$, $1/\chi$ follows the Curie-Weiss law above 30 K with a paramagnetic temperature $\theta_p = -41$ K. The molar Curie constant corresponds to a moment $\mu = 3.74\ \mu_B$ which is somewhat lower than the spin only value of 3.87 μ_B for the Cr^{3+} ion. Difference patterns obtained from neutron diffraction patterns at 5.9 and 77 K show no trace of superlattice Bragg peaks due to antiferromagnetic ordering of the spins on the Cr-ions.

This is at present interpreted as being due to the random arrangement of the metal ions.

Magnetic Form Factor in Fe at Small Wave Vectors Determined by Intensity Study of Inelastic Magnetic Neu' on Scattering

(J. Als-Nielsen and G. Shirane (Brookhaven National Laboratory, U.S.A.))

Bragg scattering data for the magnetic form factor $f(\varkappa)$ in Fe have previously been interpreted by assuming a magnetic moment distribution from 3d electrons carrying 2.39 μ_B/atom superimposed on an oppositely polarized sea of 4s electrons carrying -0.21 μ_B/atom. We have attempted to observe this directly by comparing the inelastic critical scattering around the forward direction with that around the (1,1,0) Bragg point using a 3-axis crystal spectrometer in the constant Q-mode of operation. We find indeed that $f(\varkappa)$ is bigger than unity at small wave vectors, $\varkappa$, having an approximately constant value of 1.06 for $0.05\ \text{Å}^{-1} < \varkappa < 0.17\ \text{Å}^{-1}$. We have not yet been able to obtain results at smaller values where a decrease of $f(\varkappa)$ towards unity is to be expected.

In addition, the unusual focusing effects in small angle inelastic scattering have revealed a central peak in the ω-spectrum slightly below T_c which we interpret as being the first observation of longitudinal critical fluctuations in Fe.

The Magnetic Form Factor of Pr Metal

(B.D. Rainford (Imperial College, London), F.A. Wedgwood (AERE Harwell, England) and B. Lebech)

Earlier magnetization and neutron diffraction measurements have shown Pr to have a singlet crystal-field ground state at both the cubic and hexagonal sites of the dhcp structure. No long-range magnetic order has been detected in single crystals down to 1.7 K. However, sizeable magnetic moments (μ_c, μ_h) may be induced at both sites by applying a magnetic field along a $\langle 1,1,0 \rangle$ reciprocal vector.

We have measured the magnetic contribution to Bragg reflections in a single crystal with an applied field of 1.57 T at 4.2 K, using one of the Harwell polarized neutron spectrometers. Some 72 distinct reflections have been measured in both the zeroth layer ((h,0,ℓ) types) and first layer ((h,1,ℓ) types), out to $\sin\theta/\lambda = 0.8\ \text{Å}^{-1}$. Reflections of the type (n,0,4m), where n and m are integers, have flipping ratios very close to unity.

This means that the $\mu_h f_h = 2\mu_c f_c$, to a very good approximation. This relationship has been used to place all the other measured magnetic structure factors on the same scale. The data for (h,0,ℓ) type reflections show only a small amount of anisotropy, though there are considerable differences at low angles between equivalent reflections in the zeroth and first layer. The data have been compared with calculation using the formalism of Balcar et al.[4] and the ground state wave function derived from an analysis of the magnetic properties of Pr. The shape of the experimental form factor (fig. 3) does not agree with calculation using the non-relativistic radial integral of Blume, Freeman, and Watson (BFW), being more sharply peaked towards small scattering vectors. A preliminary analysis indicates that the radial wave function in the metal is expanded by about 12% compared to the non-relativistic calculation. Similar discrepancies have been noticed previously for the heavy rare-earth metals Gd, Tb, and Tm.

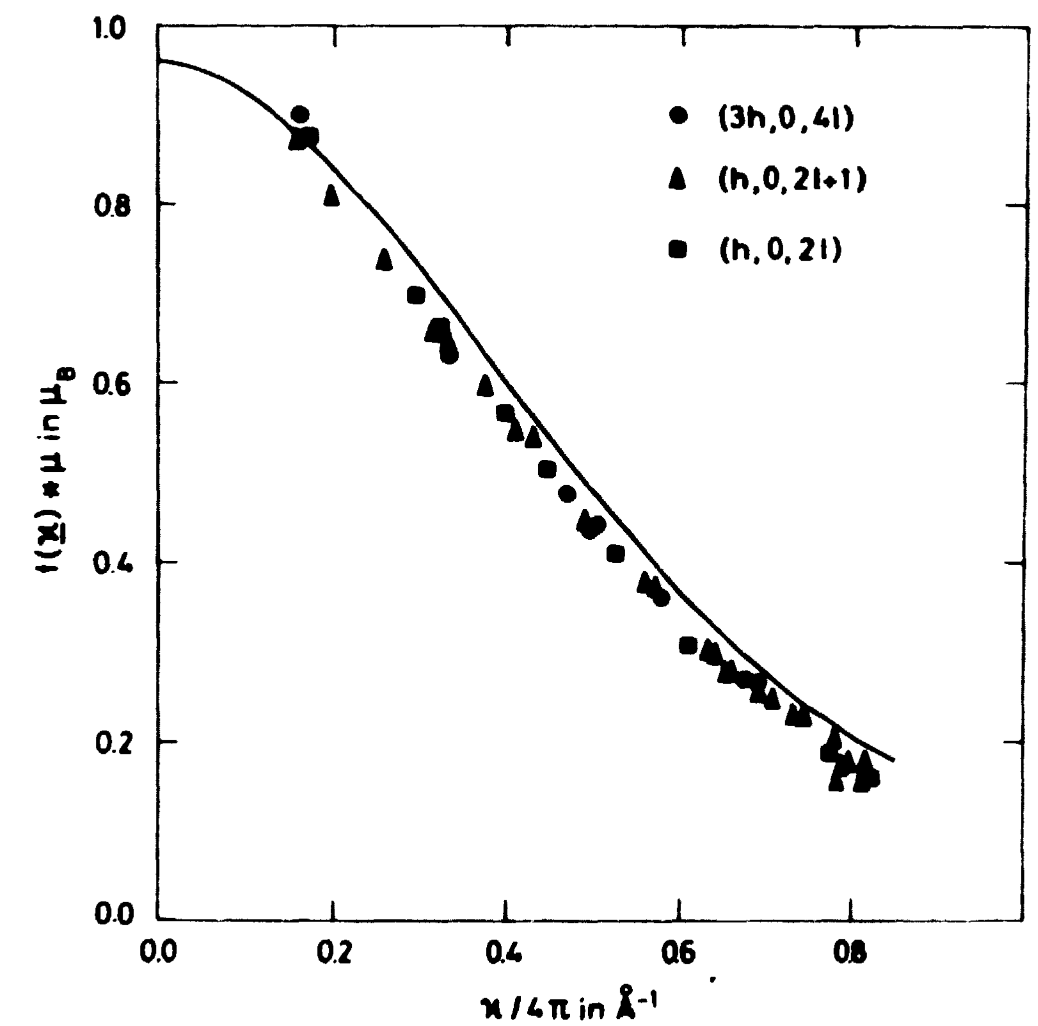

Fig. 3. Magnetic form factor $f(\varkappa)$ of Pr metal in the zeroth layer as derived from the flipping ratios. The data have been corrected for the non-ideal flipping efficiency, depolarization in the sample, and the half-wavelength contamination. The solid line shows $\mu \times f(\varkappa)$ calculated in the dipolar approximation using the HFW wave functions and the bulk magnetization value 0.96 μ_B of the moment per site.

[4] E. Balcar, S.W. Lovesey, F.A. Wedgwood, J. Phys. C3, 1292 (1970)

Theory of Pr Metal

(P.-A. Lindgård)

The Pr^{3+} ion on the hexagonal sites in the dhcp structure has a singlet ground state $|0\rangle$. The symmetric and anti-symmetric states $|1s\rangle$ and $|1a\rangle$ respectively, are not mixed with other states and are directly observable with neutron scattering. They are non-degenerate at finite wave vectors owing to two-ion-anisotropy, as discussed by Lindgård and Houmann[5]. At high magnetic field a component from the $|3s\rangle$ or $|3a\rangle$ states becomes ground state. However, the zero field energy of this state is not well determined. A molecular field calculation shows that it may vary from twice to half the separation between the $|0\rangle$ to $|1s, 1a\rangle$ state (~30 K) and still be consistent with the field measurements and the specific heat measurements. A slightly better fit is obtained when it is at twice the energy (~60 K) in accordance with Rainford's[6] analysis. At low temperatures the system therefore reduces to an effective spin 1 system. A theory for the dispersion and the temperature variation of the $|1s, 1a\rangle$ levels has been developed using a decoupling scheme based on a free energy principle.

Magnetic Excitons in Pr Metal

(J. G. Houmann and A. R. Mackintosh, B. D. Rainford (Imperial College, London), D. McMasters, and K. A. Gschneider (Iowa State University, U. S. A.))

Using a large single crystal, grown at Iowa State University, we have performed further neutron scattering experiments on the magnetic exciton dispersion relations in paramagnetic Pr. The new results generally agree with those reported earlier[7] but are considerably more detailed and precise. Fig. 4 only shows the excitation energies on the hexagonal sites, corresponding to the transition from the ground state $J = |0\rangle$ to the $J = |1a, 1s\rangle$ excited crystal field level. Except along the c-direction and at the

[5] P.-A. Lindgård and J.G. Houmann, Conference Digest No. 3, Rare Earths and Actinides, Durham, 192 (1971)

[6] B. D. Rainford, 17th Annual Conference on Magnetism and Magnetic Materials, Chicago, AIP Conference Proceedings 5, 591 (1971)

[7] B. D. Rainford and J. C. G. Houmann, Phys. Rev. Letters 26, 1254 (1971)

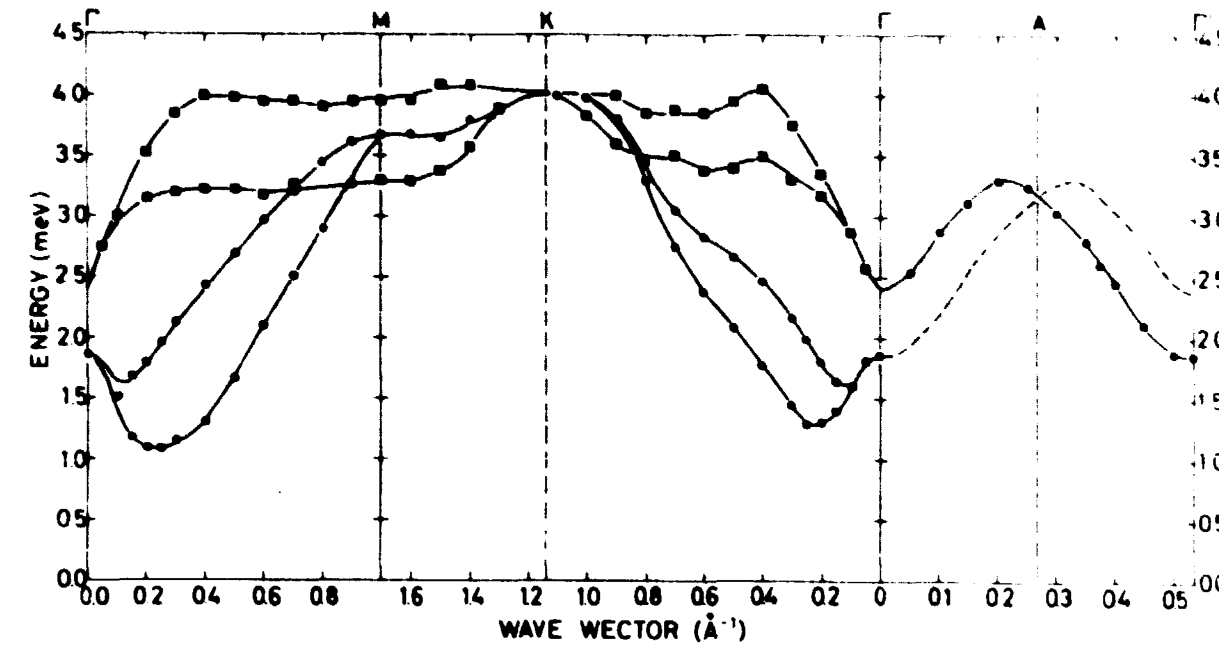

Fig. 4. Excitation energies on the hexagonal sites of Pr metal at 6.4 K.

K-point the $|1s, 1a\rangle$ level is split by anisotropic exchange, in qualitative agreement with the results of Lindgård and Houmann[5]. A careful study of this splitting and of the intensities of the associated modes allows an explicit determination of the anisotropic exchange, whose magnitude is comparable to that of the isotropic exchange. In[5] it was pointed out that by a suitable choice of scan it is possible to distinguish between the two modes associated with J^x and J^y respectively. It was shown experimentally that by performing a scan in which the direction of the scattering vector is along the ΓK direction (X direction) the lower of the two upper modes is extinguished. The theory then allows us to associate this mode with J^x. In the same way the lowest mode along the ΓM direction can be associated with J^y.

The minimum in the dispersion relation occurs along ΓM, at a point in κ-space ($q \sim 0.25$ Å^{-1}) which corresponds to the modulation vector, Q, describing the magnetic order of Pr-5.6% Nd[8]. This mode decreases substantially in energy as the temperature is reduced from 30 to 6 K and the lifetime of the excitations simultaneously increases. It is expected that if Pr orders magnetically then this mode will decrease to zero ("go soft") at the ordering temperature. In order to investigate this, it is planned to study the energy of the mode as a function of temperature in the range 6 - 1.2 K in the near future.

[8] B. Lebech, Risø Report No. 258, 14 (1972)

Magnetic Structures of Nd in Strong Magnetic Fields

(B. Lebech and B. D. Rainford (Imperial College, London))

Nd has the double hexagonal close-packed structure in which there are two types of sites with local cubic and hexagonal environment respectively. The magnetic ordering on the two sites in zero magnetic field has previously been described by a simple model. In terms of this model the moments on the hexagonal sites order at 19.2 K along $\underline{b}_1$ in a modulated antiferromagnetic structure with modulation vector $\underline{Q}_h$. At 7.8 K the moments on the cubic sites order similarly along $\underline{b}_2$ with modulation vector $\underline{Q}_c$. The onset of ordering on the cubic sites induces a change in the ordering on the hexagonal sites.

To explain some discrepancies between the intensity effects produced by this magnetic structure model and those observed by neutron diffraction we suggest like Moon et al.[9] that exchange interactions between the atoms on the hexagonal sites induce a modulated moment, μ_{cm}, on the cubic sites with ferromagnetic coupling between neighbouring layers of cubic atoms. We further suggest that dipolar forces give rise to an antiferromagnetic component of the induced moment as well. In addition, the induced moment is turned towards the easy $\underline{b}_2$ direction in the cubic layers, because of single-ion anisotropy. The results are now being analysed in terms of this model.

Fig. 5 shows typical results obtained for the intensity versus field dependence of the satellites corresponding to the $\underline{Q}_c$ and $\underline{Q}_h$ modulation vectors. Above 0.8 T ferromagnetic moments develop at both the cubic and the hexagonal sites. The behaviour of the $\underline{Q}_c$ satellites is consistent with a uniform distribution of domains in zero field followed by the formation of a single cubic domain with $\underline{Q}_c$ perpendicular to the field at 0.8 T and with complete ferromagnetic alignment of the cubic moments in the applied field at 3.2 T. This interpretation leads to a drop of about 0.4 μ_B in the modulated moment due to the $\underline{Q}_c$ modulation at 0.8 T and a corresponding increase in the ferromagnetic moment on the cubic atoms. The transition observed at 0.8 T corresponds to an anomaly observed in the magnetization measurements. The ferromagnetic moments increase steadily until 2.6 T when we observe an abrupt increase in the induced ferromagnetic moments of about 0.8 μ_B on both sites. The intensity variations due to $\underline{Q}_h$ are more complex and the results are still being analysed.

9) R. M. Moon, J. W. Cable, and W. C. Koehler, J. Appl. Phys. 35, 1041 (1964)

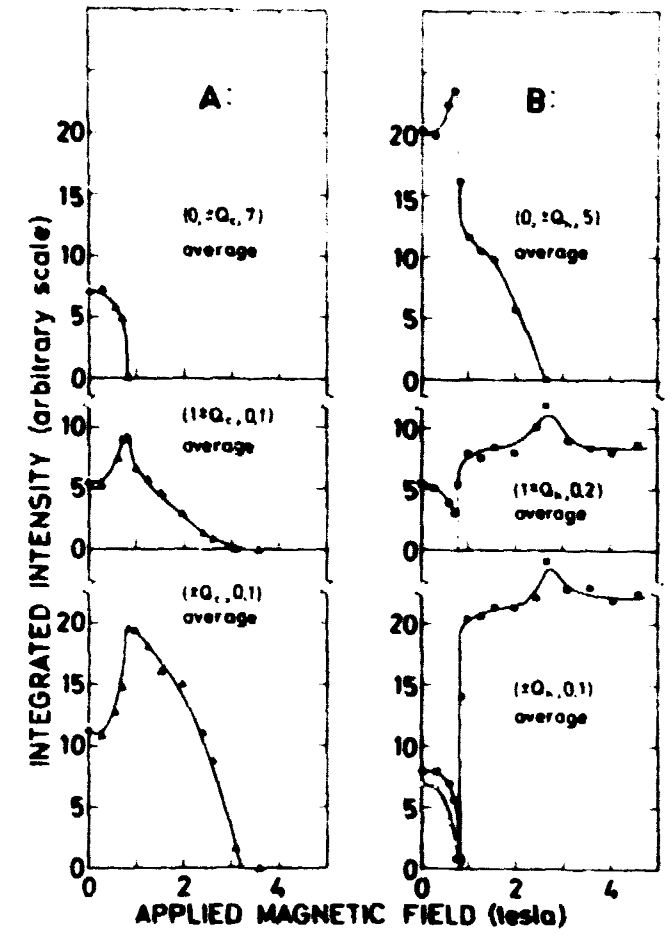

Fig. 5. Intensity variations of the magnetic satellites in Nd when a magnetic field is applied along a $[1,\bar{2},1,0]$ direction.
A) Satellites due to $\underline{Q}_c$ parellel to equivalent $[1,0,\bar{1},0]$ directions and μ_{cm} parallel to equivalent $[1,1,\bar{2},0]$ directions. The anomaly in the $(1 \pm Q_c, 0, 1)$ satellites at 0.8 T indicates that the modulated moment due to $\underline{Q}_c$ is turned towards $\underline{Q}_c$.
B) Satellites due to $\underline{Q}_h$ parellel to equivalent $[1,0,\bar{1},0]$ directions.

Crystal-Field Splitting in $PrFeO_3$

(K. Hennig (Dubna, USSR) and E. Warming)

The Pr ion in $PrFeO_3$ is trivalent and the free ion ground state of Pr^{3+} is a $^3H_4$ multiplet with nine non-degenerate levels. By inelastic neutron scattering in a powder sample we have studied three transitions at three temperatures; 4, 10, and 77 K. The levels determined are: $E(\Gamma_3') = 0$ meV, $E(\Gamma_3'') = 2.2$ meV, $E(\Gamma_5) = 15$ meV, and $E(\Gamma_4) = 26$ meV. For an ion in a crystal-field potential of cubic point symmetry the Hamiltonian may be described by only the fourth and sixth order terms in a Stevens operator expansion. Lea, Leask, and Wolf[10] defined a crystal-field parameter, x,

10) K. R. Lea, M. J. M. Leask, and W. P. Wolf, J. Phys. Chem. Solids 23, 1381 (1962)

as the ratio between the coefficients to these two terms. From the measured energies we deduced $x = 0.57$. (To be published in Phys. Status Solidi).

Crystal-Field Splitting in Nd-Chalcogenides

(P. Bak, A. Furrer (EIR Würenlingen, Switzerland), P.-A. Lindgård, and E. Warming)

The effort to map the crystal-field splitting in metallic rare-earth compounds was continued. The three Nd-chalcogenides: NdS, NdSe, and NdTe were studied, at 4, 77, and 300 K. A preliminary analysis based on the observed transitions gives the following crystal-field parameters[10], x, at room temperature: x(NdS) = 0.69, x(NdSe) = 0.69, and x(NdTe) = 0.62.

Magnetic Properties of Nd-Group V Compounds

(P. Bak, P.-A. Lindgård, and E. Warming)

The Nd-monopnictides NdP, NdAs, and NdSb are simple cubic type I antiferromagnets in which the crystal-field splitting is larger than the exhange energy. The magnetic properties were calculated using wave functions determined by inelastic neutron spectroscopy. A mean-field theory including crystal-field and magneto-elastic effects was developed. The magneto-elastic coupling acts as an effective second-order two-ion interaction. The total single-ion Hamiltonian may thus be written as

$$H = V_C - 2J(0)\langle J^z\rangle J^z - 2K(0)\langle O_o^2\rangle O_o^2$$

The temperature dependence of the magnetostriction is obtained by solving this Hamiltonian self-consistently and it agrees with experiments for NdSb[11]. Until now, the magnetostriction has not been measured in NdP and NdAs. However, the quenching of the magnetic moment is only partly understood from the present theory.

Contrary to the above-mentioned compounds, NdN orders ferromagnetically. Inelastic neutron scattering experiments on this compound are in progress. By comparison with experimental results on PrN, the crystal-field splitting of NdN is expected to be larger than for the antiferromagnetic Nd-monopnictides.

---

11) F. Levy, Phys. Kond. Mat. 10, 85 (1969)

Magnetic Properties of Rare-Earth-Al_2 Compounds

(P. Bak and H.-G. Purwins)

The magnetic properties of the rare-earth compounds $TbAl_2$, $ErAl_2$, and $NdAl_2$ were calculated using crystal-field parameters determined by inelastic neutron scattering and susceptibility measurements. The theoretical spontaneous magnetization agrees with experiments. A two-dimensional mean-field theory was developed to calculate magnetization curves for external magnetic fields in symmetry directions other than the easy direction. The field turns the magnetic moment towards hard directions, but at the same time the quenching is partly removed, so that the magnetization differs from that calculated in a semi-classical anisotropy theory[12]. Experimental magnetization curves[13,14] are reproduced within 10%.

Collective Excitations in Magnetic Systems with Strong Crystalline Electric Fields

(P. Bak)

A temperature dependent Green function method was developed to calculate dispersion relations for magnetic excitations in magnetic systems in which crystal field effects are important. The method can be applied to systems with two-ion interactions of arbitrary order. The Green functions involve operators creating transitions between single-ion crystal field or molecular field states. The equations of motion of the Green functions are decoupled in either a random phase approximation or in a generalized Callen approximation[15] taking into account two-ion correlation effects. In the first case the theory is identical to Grover's[16] pseudo-Bose theory in the low-temperature limit, and it reproduces the excitation spectrum derived by Peschel et al.[17] at all temperatures. Neutron cross sections can be determined directly from the residues of the Green functions. The theory has been used to interpret the excitation spectra of $NdAl_2$ and $TbAl_2$.

---

12) G.T. Trammel, Phys. Rev. 131, 932 (1963)
13) B. Barbara, M. Rossignol, E. Walker, and H.-G. Purwins, to be published
14) H.-G. Purwins, Z. Phys. 233, 27 (1970)
15) H.B. Callen, Phys. Rev. 130, 890 (1963)
16) B. Grover, Phys. Rev. 140, A1944 (1965)
17) I. Peschel, M. Klenin, and P. Fulde, J. Phys. C5, L194 (1972)

Dispersion Relations for Magnetic Excitons in $NdAl_2$

(J.G. Houmann, P. Bak, H.-G. Purwins, and E. Walker (Université de Genève))

$NdAl_2$ is a magnetic system in which the exchange field and the crystalline electric field are of the same order of magnitude. At 4.2 K, the crystalline electric field is strong enough to cause considerable quenching of the spontaneous magnetic moment. Thus, the moment is reduced to 75% of the free ion value. The magnetic excitations in such systems differ substantially from the spin waves occurring in magnets with vanishing crystal fields. The excitations are transitions between combined crystal field and exchange field single-ion levels propagating through the lattice via the exchange interaction.

$NdAl_2$ is particularly well suited for both theoretical calculations and experiments especially as (1) the local symmetry of the magnetic Nd^{3+} ion is cubic, which limits the number of independent crystal field parameters to two. This facilitates theoretical considerations greatly and reduces the number of excitation branches which can be measured by neutrons; and (2) large single crystals are available. This allows us to determine the dispersion relations over all the Brillouin zone. We are thus not limited to spherical averaged dispersion relations, as was the case with previous measurements on powder samples of fcc Pr, Pr_3Tl, and rare-earth-group V compounds.

The dispersion relations measured by inelastic neutron scattering are presented in fig. 6. The two lower branches are excitations between the two states originating from a Γ_6 crystal field ground state doublet. The upper branches are excitations between the ground state and higher mean-field states. Theoretical calculations were performed in the RPA approximation using a Hamiltonian which includes a cubic crystal field term and a Heisenberg exchange interaction term. The agreement between theory and experiment seems to indicate that $NdAl_2$ is a model system for this simple Hamiltonian. The longitudinal acoustic and optical branches (LO, LA) originate from the $S_i^z \cdot S_j^z$ part of the exchange interaction, the transverse spin wave-like branches (TO, TA) from the $S_i^+ S_j^-$ part.

Further measurements are planned to improve the resolution of the different branches and to determine the dispersion of the crystal field levels in the paramagnetic regime.

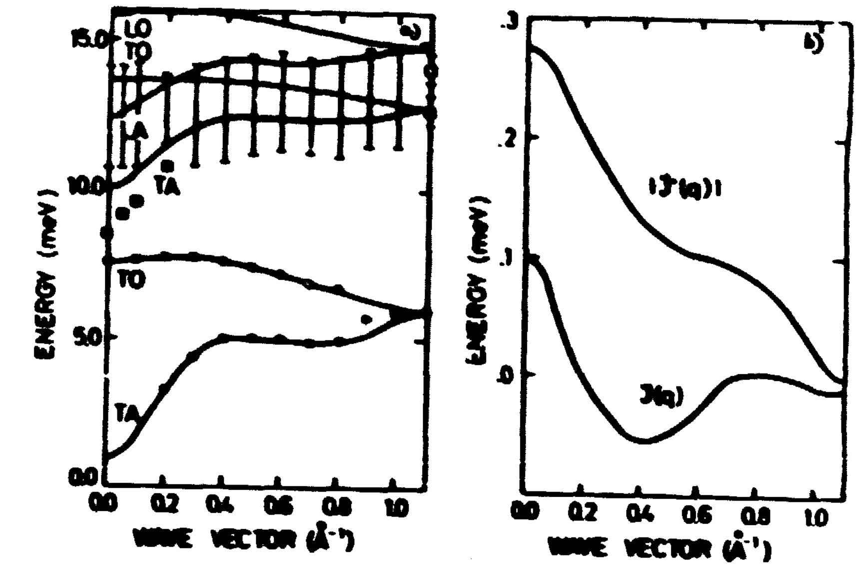

Fig. 6. Dispersion relation for $NdAl_2$ measured by inelastic neutron scattering.

Magnon - Exciton Interaction in $TbAl_2$

(J.G. Houmann, P. Bak, H.-G. Purwins, and E. Walker (Université de Genève))

A hitherto unobserved effect, the magnon-exciton interaction, has been observed in $TbAl_2$ by inelastic neutron scattering measurements of the energies of the magnetic excitations.

The measured temperature dependence of the magnetic excitation energies is shown in fig. 7. The striking feature of the spectrum is the appearance of an additional peak in the scattered neutron intensity at about 30 K. The double-peak structure may be explained quantitatively by using a Hamiltonian which includes a cubic crystal field term and an isotropic Heisenberg interaction term. The calculations were carried out by means of a temperature dependent Green function method in the RPA approximation.

At low temperatures the single exciton branch can be described as an ordinary spin wave branch. As the temperature is raised, the renormalized magnon energy approaches and crosses the energy difference between the high-lying single-ion states $|1\rangle$ and $|2\rangle$. This gives rise to mixing of the magnon with the exciton corresponding to the transition from $|2\rangle$ to $|1\rangle$. This causes anti-crossing effects in analogy with for example the magnon-phonon interaction. The magnetic exciton is thus observed through the magnon - exciton interaction in spite of the extremely low population of the corresponding single-ion states.

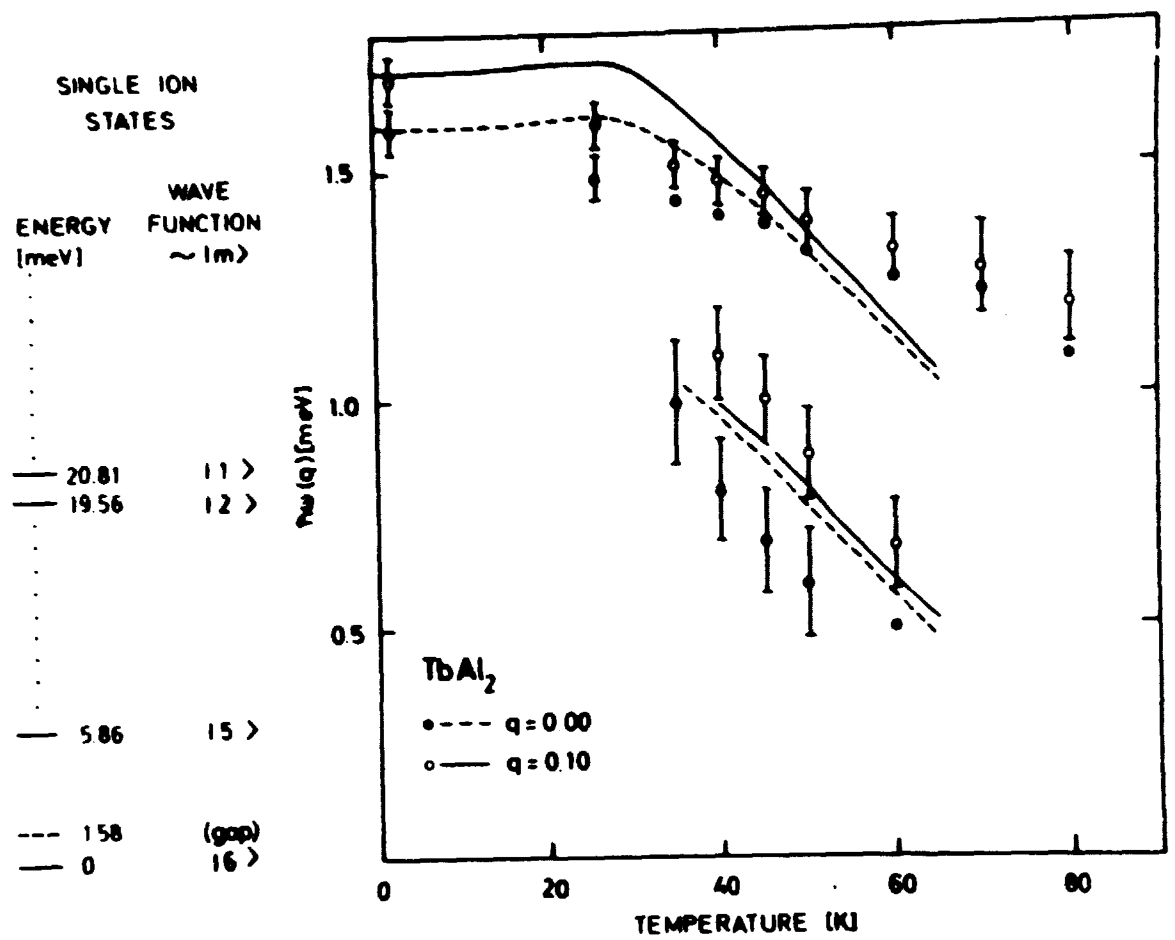

Fig. 7. Temperature dependence of the magnetic excitation energies in $TbAl_2$. The full and dotted lines are calculated by a temperature dependent Green function method in the RPA approximation.

Magnetic Impurities in CoF_2

(R. A. Cowley and O. W. Dietrich)

We have studied the effect on the spin wave spectrum of diluting the magnetic insulator CoF_2 with large amounts of non-magnetic ions of Zn. Two crystals, with 25% Zn and 50% Zn, were investigated at Risø. Large concentrations of Zn can be substituted for Co in these crystals without causing any change in the crystal structure, but there is a marked change in the magnetic excitations. The effect of dilution is to decrease the energy and the lifetime of the spin waves. The results are now being analyzed as part of a series of measurements which include a sample of 75% Zn and the results on pure CoF_2[18].

[18] R. A. Cowley, W. J. L. Buyers, P. Martel, and R. W. H. Stevenson, J. Phys. C6, 2997 (1973)

Spin Waves in EuO and EuS

(O. W. Dietrich, J. Als-Nielsen, and L. Passell (Brookhaven National Laboratory, U. S. A.))

The measurements of the spin wave dispersion in EuO and EuS using the neutron scattering technique at the Brookhaven High Flux Reactor revealed exchange constants between nearest neighbours (nn) and next-nn Eu-ions in EuO which disagreed with the results previously obtained by various authors using the specific heat and the NMR techniques. We have reanalysed the bulk measurements which were made below 4.2 K. The analysis shows that below 4.2 K both the specific heat and the NMR are insensitive to the particular values of the exchange constants, but only depend on their sum. This is so because only spin waves of wave vectors in the parabolic region near the zone centre of the Brillouin zone are populated below 4.2 K. The new analysis brings the bulk results in agreement with our scattering results for EuO. In EuS, there was only a minor disagreement between the different measurements, because the Curie temperature in EuS is only 16.6 K (69.2 K in EuO). This means that already at 4.2 K there is a significant population of spin waves for wave vectors throughout the Brillouin zone.

Spin Wave Dispersion and Sublattice Magnetization in $NiCl_2$

(P.-A. Lindgård, J. Als-Nielsen, and R. J. Birgeneau (Bell Laboratories, U. S. A.))

$NiCl_2$ is a near-Heisenberg planar antiferromagnet composed of hexagonal ferromagnetic Ni^{++} sheets with effective X-Y symmetry weakly coupled antiferromagnetically to adjacent Ni^{++} sheets. The almost two-dimensional characteristics imply an unusual spin wave renormalization and sublattice magnetization. A theory for these properties, which does not contain any assumptions about the temperature dependence of the energy gap, has been developed. The dispersion for spin waves propagating in the plane has been measured by means of neutron scattering, and data for the low, out-of-plane spin wave energies have been obtained. Also the sublattice magnetization versus temperature has been measured. Comparison of the experimental data with the theory yields the following values for the exchange interaction in the plane $J_{nn} = 21.7$ K, $J_{nnn} = -4.85$ K, and between the planes $J' = 0.85$ K. The planar anisotropy constants obtained by a similar comparison are $D = 0.43$ K and $D' = 0.41$ K.

Spin Waves in Tb. I: Magnetic Anisotropy

(J.G. Houmann, J. Jensen, and P. Touborg (Technical University of Denmark))

The study of magnetic anisotropy in Tb, obtained from the field dependence of the spin wave energy gap, was continued. The experimental results were corrected for the influence of the field dependence of the relative magnetization. This correction gives rise to modifications of the temperature dependence of the anisotropy parameters obtained in[19].

With the exception of the sixfold basal plane anisotropy, the anisotropy parameters deduced from our results agree with macroscopic measurements[20] both in magnitude (at zero temperature) and in the temperature dependence. The different results for the sixfold anisotropy may be due to the presence of polarization-dependent two-ion couplings in the spin Hamiltonian. These couplings contribute differently to the spin wave measurements and to the macroscopic measurements. The anisotropy parameter, ΔM (defined in[19]) which is quite large, is probably also of two-ion origin and is presumably connected with the exchange anisotropy observed in Tb.

Spin Waves in Tb. II: Magnon - Phonon Interaction

(J. Jensen and J.G. Houmann)

The interaction between the spin waves and the transverse phonons propagating in the c-direction of Tb influences strongly the field dependence of the spin wave energies. The magnons interact simultaneously with the acoustic and optical phonons. The equations of motion for this system were solved. Because of the antisymmetric character of the abnormal (acoustic to optical) coupling this interaction vanishes at zero wave vector ($\propto q^2$). In spite of the indirect coupling of the acoustic and optical magnons via the phonons, the magnons remain double degenerate at the Brillouin zone ($q = \pi/c$). This behaviour of the magnon - phonon interaction is to some extent supported by experimental measurements. The strength of the couplings between the magnons and the phonons (as functions of the wave vector) was deduced by combining experimental studies of the mode mixings with theoretical considerations.

---

19) H. Bjerrum Møller, J.C.G. Houmann, J. Jensen, P.-A. Lindgård, M. Nielsen, and A.R. Mackintosh, Risø Report No. 256, 223-232 (1972)

20) J.J. Rhyne, Magnetic Properties of Rare Earth Metal (R.J. Elliot Editor), Plenum Press, London (1972)

Spin Waves in Tb. III: Anisotropic Exchange Interaction

(J. Jensen, J.G. Houmann, and H. Bjerrum Møller)

The study of the field dependence of the energies of spin waves propagating in the c-direction of Tb was continued. The experimental results were corrected for the perturbation due to magnon - phonon interaction and for the influence of the field dependence of the relative magnetization, σ. The two perpendicular components of the anisotropic two-ion coupling between the moments were deduced as a function of wave vector, of relative magnetization, and of the direction of the magnetization in the basal plane.

The different kinds of two-ion couplings obtained in Tb have been classified by means of a general two-ion spin Hamiltonian:

$$H_{MJJ} = \frac{1}{2} \sum_{ij} \sum_{\gamma\tau} \sum_{lm} \sum_{l'm'} K_{\gamma ll'}^{\tau mm'}(\underline{R}_i - \underline{R}_j) \langle \tilde{O}_{\gamma\tau} \rangle \tilde{O}_{lm}(J_i)\tilde{O}_{l'm'}(J_j)$$

$$+ \text{ hermitian conjugate}$$

where $\tilde{O}_{lm}(J_i)$ are Racah operators and J_i is the total angular moment on the site $\underline{R}_i$. From this Hamiltonian a general expression for the spin wave energies in Tb was deduced and compared with the energies obtained experimentally.

The anisotropy deduced from the neutron measurements shows the following behaviour. At 4.2 K the axial anisotropy, describing the difference between the c-axis and the basal plane components of the exchange interaction, amounts to about 30% of the isotropic part. It decreases rapidly with the relative magnetization. A difference between the components of the exchange interaction in the easy and in the hard direction, which is comparable in magnitude to the axial anisotropy, has been observed. The rapid decrease of both the axial and basal plane anisotropy (both of which are proportional to σ^{12}) implies that the exchange interaction is effectively isotropic above 150 K.

Anisotropic Exchange Interaction in the Conical Magnetic Phase of Er

(J. Jensen)

From a general two-ion Hamiltonian we deduce an expression for the energies of spin waves propagating in a hexagonal solid in which the magnetic moments are ordered in a conical or helical structure. The spin wave dispersion relation in the c-direction of Er in its conical magnetic phase at 4.5 K, which has been studied by Nicklow et al.[21], is reanalysed. In this analysis we introduce an alternative kind of anisotropic coupling between the total angular moments on the sites i and j, proportional to the following combination of Racah operators: $\tilde{O}_{2,+2}(J_i)\,\tilde{O}_{2,-2}(J_j)$, expressed with respect to a co-ordinate system with the z-axis along the c-direction. The resulting anisotropy is reduced by an order of magnitude in comparison with that deduced by Nicklow et al.[21]. The constant part of the anisotropy is found to be equal to about 20 meV (a rough estimate from magnetization measurements gives 5-10 meV). The wave vector dependent part of the exchange interaction is found to be of the same order of magnitude as the isotropic part.

Electronic Structure of hcp Metals - Application to Yb

(O. Jepsen and O. Krogh Andersen)

An intuitively simple and computationally fast approach to electronic energy bands and wave functions[22] is being applied to hcp crystals with hexagonal close-packed structure, in particular Yb.

In the simplest version of this scheme the eigenvectors A_{lj} (l = s, p and d; j = {m, q} = -Nl, Nl) satisfy the homogeneous linear equations in angular momentum representation

$$\sum_{l,j} \{-p_l(E)\delta_{l'l}\delta_{j'j} + S^{\underline{k}}_{l'j';\,lj}\} A_{lj} = 0 \qquad (1)$$

if the energy is E and the Bloch vector $\underline{k}$. N is the number of like atoms in the primitive cell. The $p_l(E)$ are increasing functions of E. These parameters only depend on the crystal potential in the atomic sphere and they may be evaluated even from atomic eigenvalues and wave functions. The structure constants $S^{\underline{k}}_{l'j';\,lj}$ are independent of the energy, the potential, and the lattice constant, and for l' = l they are diagonal in j. Consequently, the diagonal elements $S^{\underline{k}}_{lj}$ form "canonical" bands, which may be computed once and for all for a given structure, and in terms of which the unhybridized energy band structure $E^{\underline{k}}_{lj}$ for a given potential follows from the implicit

[21] R. M. Nicklow, N. Wakabayashi, M. K. Wilkinson, and R. E. Reed, Phys. Rev. Letters 27, 334 (1971)

[22] O. K. Andersen, Solid State Commun. 13, 133 (1973) and O. K. Andersen, Transition Metals, Alloys and Magnetism (Mont Tremblant International Summer School, 1973 (unpublished))

equation $p_l(E) = S^{\underline{k}}_{lj}$. The 10 canonical d-bands of the hcp-structure with c/a = 1.673 are shown in fig. 8. Inclusion of the s-p-d- hybridization requires the solution of (1) or a transformed set of equations having the form characteristic of the eigenvalue problem. In this form perturbations like non-spherical contributions to the cellular potential are easily included. To obtain all 18 eigenvalues per $\underline{k}$-point in the hcp structure with our present computer codes, which include relativistic effects and a non-spherical correction to the potential, we use 20 seconds on the Burroughs B 6700. If spin-orbit coupling is neglected and only the 4 lowest eigenvalues are needed, the computing time is 2 seconds. When compared with fully converged APW energies using the same Yb-potential, the root mean square error of our approach is 3 mRy and the maximum error, for 200 energies, is 9 mRy.

We have investigated a possible origin of the hcp to fcc phase transition of the divalent rare-earth metal Yb by computing the pressure dependence of the energy bands and the Fermi surface in the hcp phase. Our previous

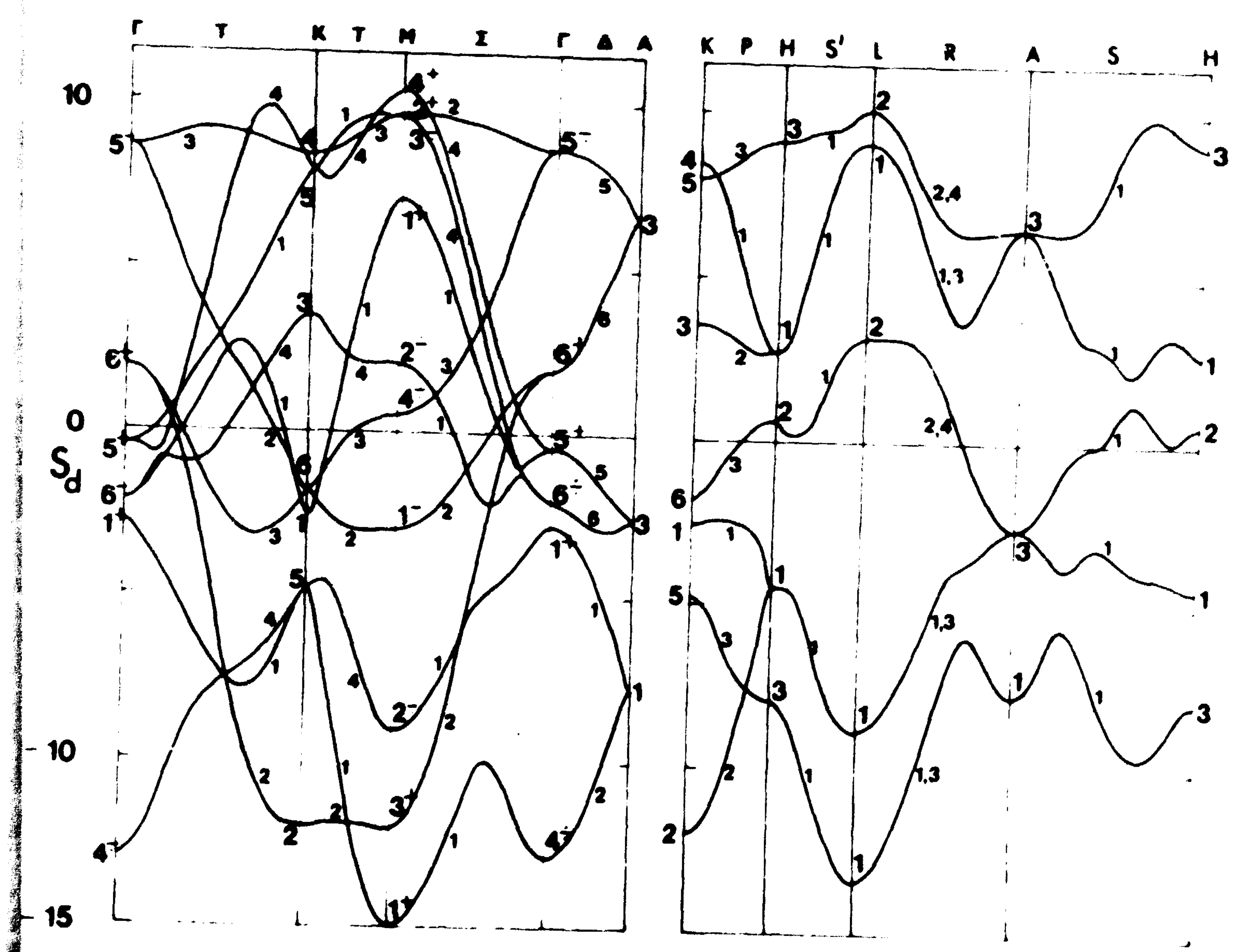

Fig. 8. The canonical d-bands for the hcp-structure.

results for the Fermi surface at normal pressure[23] were in good agreement with de Haas-van Alphen experiments, and measurements under pressure are now in progress[24]. The energy bands of the hcp rare earths are all similar, but in Yb the third band, which is responsible for two sheets of the Fermi surface, is abnormally flat and, as seen in fig. 9, the Fermi energy falls at a steep slope in the density of states. Pressure effects are pronounced because the particular flat band arises as an effect of strong hybridization between the resonant 5d and the 6d bands which depend differently on volume.

We hope that our approach to the band structure problem will permit theoretical calculations of crystal fields and exchange interactions in rare-earth metals and a study of the electronic structure of other but the simplest materials.

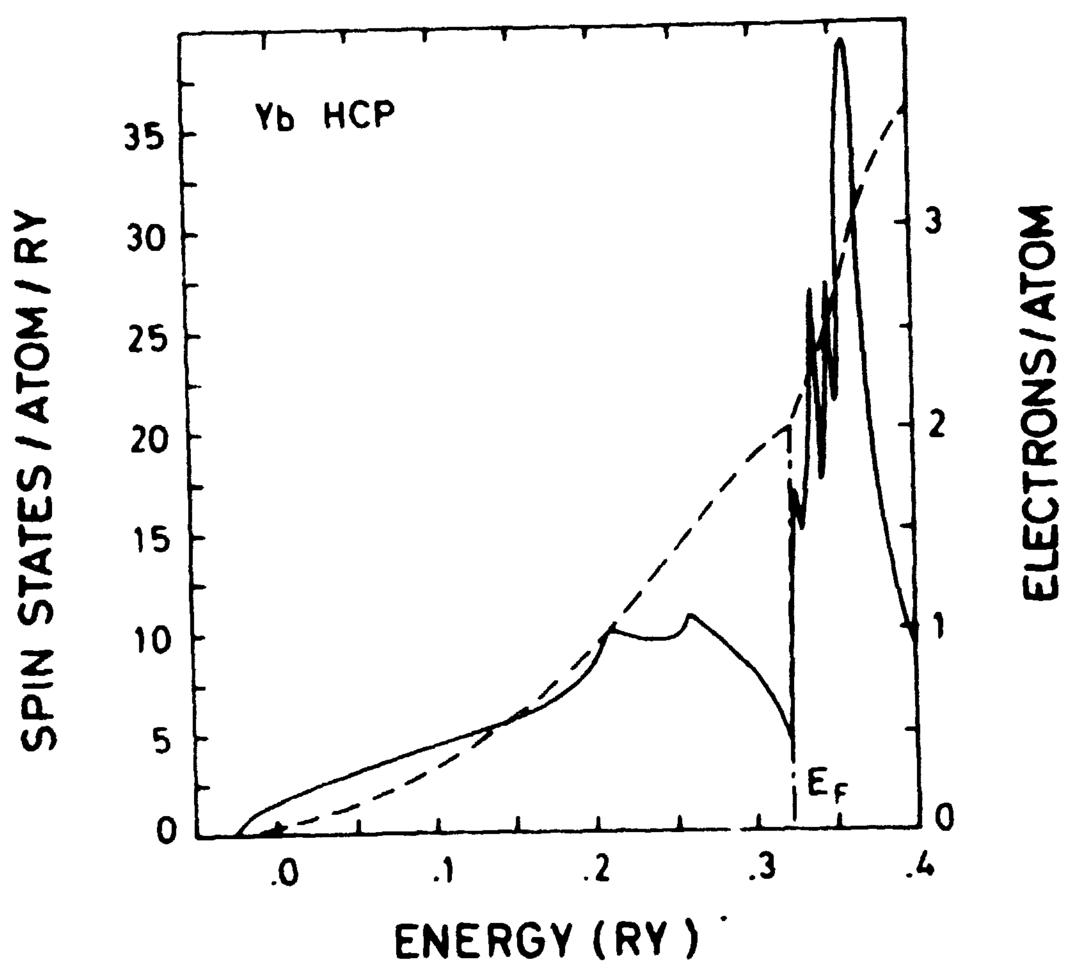

Fig. 9. The density of states (solid line) and number of states (dashed line) for hcp Yb at normal volume. The Fermi energy falls at the onset of the 5d and the 6p bands.

23) O. Jepsen, Thesis (Technical University of Denmark, 1972 (unpublished)), and O. Jepsen and O.K. Andersen, Solid State Commun. 9, 1763 (1971)

24) R. Datars and A. Slavin, private communications

Exchange Interaction in the Heavy Rare-Earth Metals Calculated from Energy Bands

(P.-A. Lindgård)

The RKKY interaction is modified in the ordered phase owing to the exchange splitting of the conduction electron bands. Using APW energy bands and a rigid band model the perpendicular and parallel susceptibilities for Gd, Dy, Tb, and Er have been calculated. The RKKY-matrix element is obtained from the wave vector dependent exchange functions which are derived from measurements. The matrix element is for all materials constant over a large part of the Brillouin zone with a narrow central peak. The exchange contribution to the free energy in the ferromagnetic phase has a clear minimum at a wave vector different from zero for Dy, Tb, and Er, but not for Gd. The spiral structure is further stabilized by the corresponding splitting of the conduction electron bands. The results are shown in fig. 10.

The calculation was performed using a "root sampling" summation. As it is difficult to assess the degree of convergence by this method, we also used a program which sums over small tetrahedra in which the energy surfaces are planar to a good approximation, and the susceptibility sum can be exactly performed. This method is an extension of that used in[23] to calculate Fermi surfaces. The result for Tb is identical to that obtained by the root sampling method, which indicates that the results shown in fig. 10 do not have significant numerical errors. The linearized method used on a test case of a spherical Fermi surface gave with 1536 tetrahedra in the reduced zone an excellent Lindhard function.

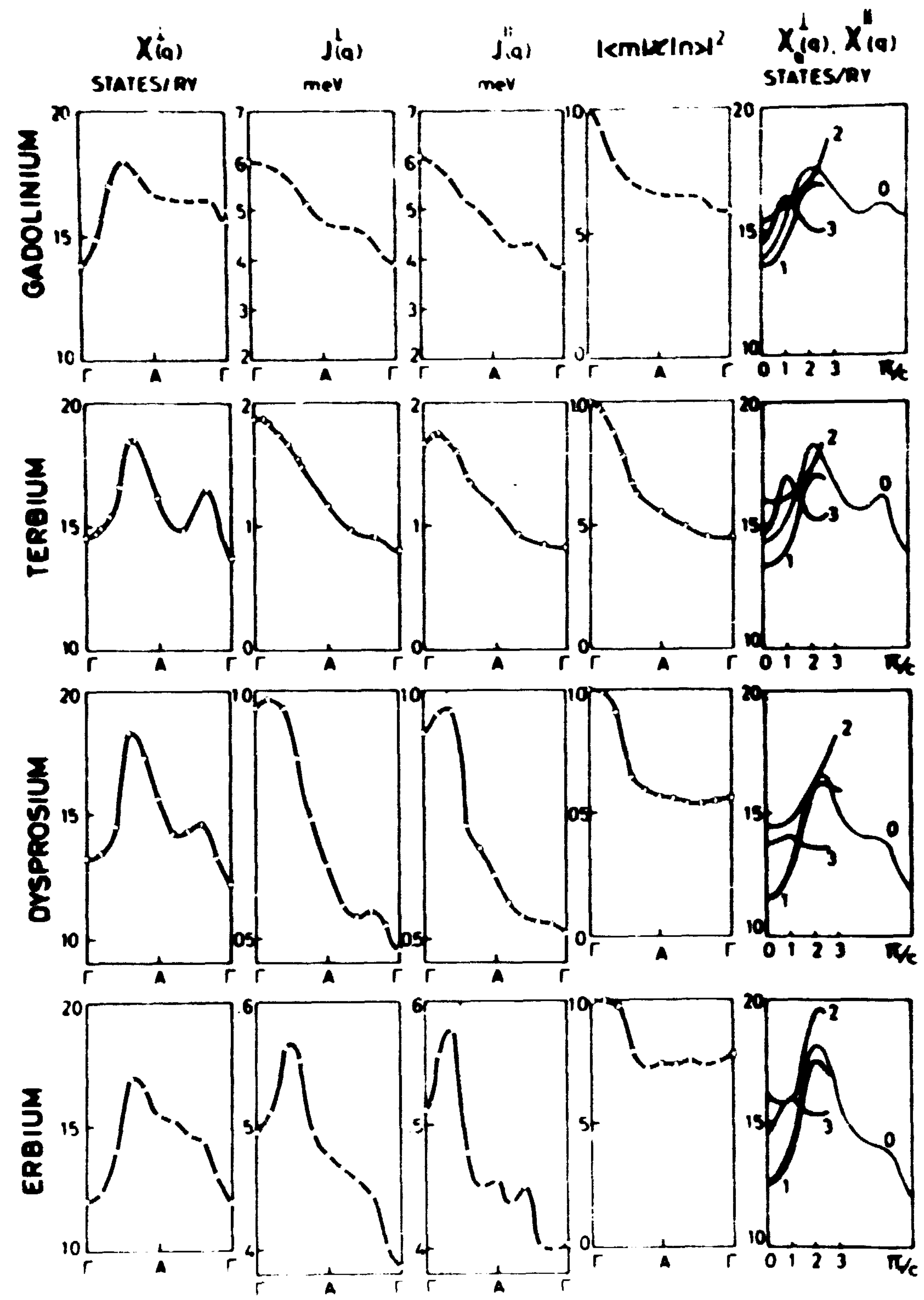

Fig. 10. The perpendicular susceptibility $\chi^{\perp}(q)$, the experimental perpendicular exchange interaction $J^{\perp}_{p'}$, the calculated parellel exchange interaction $J^{\parallel}_{p'}$, and the deduced matrix element $|j(q)|^2/|j(0)|^2 = |\langle m|H|n\rangle|^2$ for the ferromagnetic phase at full saturation (splitting: 8 mRy). The last column shows $\chi^{\perp}_{Q}(q)$ in the spiral phase for $Q_n = \frac{n\pi}{6c}$, $n = 1, 2, 3$ (splitting: 4 mRy). The ferromagnetic $\chi^{\parallel}(q)$ is shown as the thin line marked 0.

Temperature Dependence of the Ferromagnetic Resonance Energy for the Heavy Rare Earths

(O. Danielsen and P. -A. Lindgård)

The classical expression for the ferromagnetic resonance energy (spin wave energy gap) in terms of the derivatives of the free energy has been used to express the temperature dependence as a function of correlation functions of tensor operators in the Hamiltonian. The calculation is done by rotating the tensor operators in the Hamiltonian, H, to a co-ordinate

system with the z-axis along a direction specified by the polar angles θ and φ. Then the resonance energy is

$$\left(\frac{M}{g\mu_B}\hbar\omega\right)^2 = F_{\theta\theta}F_{\varphi\varphi} - F^2_{\theta\varphi} .$$

where $F_{\alpha\beta}$ are the derivatives of the free energy with respect to α and β. The derivatives are given by

$$F_{\alpha\beta} = \left\langle\frac{\partial^2 H}{\partial\alpha\partial\beta}\right\rangle + \frac{1}{kT}\left\{\left\langle\frac{\partial H}{\partial\alpha}\right\rangle\left\langle\frac{\partial H}{\partial\beta}\right\rangle - \left\langle\frac{\partial H}{\partial\alpha}\cdot\frac{\partial H}{\partial\beta}\right\rangle\right\}.$$

Temperature Dependence of the Macroscopic Anisotropy Constants in Hexagonal Systems

(O. Danielsen and P. -A. Lindgård)

The temperature dependence of single-ion anisotropy terms is investigated in the spin wave theory renormalized in the Hartree-Foch approximation. Suppose the free energy is

$$F = \sum_{n=o}^{3} K_n \sin^{2n}\theta + K_4 \sin^6\theta \sin 6\varphi ,$$

where θ and φ are polar angles specifying the direction of the magnetization and let the Hamiltonian be

$$H = H_{\text{exchange}} + \sum_{L,M} B_{LM} O_L^M(i) ,$$

where the average exchange interaction is the dominant term and $O_L^M(i)$ are Stevens operators in a general expansion of the anisotropy. The temperature dependence of the anisotropy constants $K_n(T)$ at low temperatures is then directly related to the mean values of the Stevens operators, which is found to be

$$\langle O_\ell^0(c)\rangle_T = \langle O_\ell^0(c)\rangle_o m(T)^{\ell(\ell+1)/2} \times (1 + b(T)^2)^{(\ell-1)\ell(\ell+1)(\ell+2)/16}$$

$$\langle O_\ell^2(c)\rangle_T = \langle O_\ell^2(c)\rangle_o m(T)^{(\ell(\ell+1)/2 \; -3/2)} \times b(T)$$

$$\langle O_\ell^4(c)\rangle_T = \langle O_\ell^4(c)\rangle_o \times b(T)^2$$

in terms of the reduced magnetization m(T) and a parameter b(T) which describes the ellipticity of the spin precession. At higher temperatures the angular and temperature dependence of the free energy is not express-ible in the above terms. In the spin wave theory it can be evaluated from the trace over spin wave states of exp(- H/kT). Numerical calculations for Gd, Tb, and Dy have been performed on the basis of the measured spin wave dispersion curves. The results are in excellent agreement with existing measurements of the magnetization and the anisotropy constants.

The Product of Angular Momentum Functions (Tensor Operators)

(P. -A. Lindgård)

In the theory of magnetism the product or the commutator of two angular momentum operators are often to be evaluated. By means of 3-j and 6-j symbols the product of tensor operators can generally be expressed in a series of single tensor operators. It is shown that the expansion of products of Racah or Stevens operators, working on states of total angular momentum J, can be written

$$T_{\ell'm'}\, T_{\ell''m''} = \sum_{LM} f(\ell'm', \ell''m'', LM, X)\,T_{LM}\,,$$

where the coefficient f depends on X = (J(J+1). Numerical tables of the product of Racah operators and Stevens operators of arbitrary rank up to six have been computed and will be published in a Risø Report.

Bose Operator Expansion of Tensor Operators in the Theory of Magnetism

(P. -A. Lindgård and O. Danielsen)

Using a method of matching corresponding matrix elements, a hermitian Bose operator expansion of tensor operators of arbitrary rank is derived. By the expansion all kinematic effects are transformed into dynamical inter-actions between Bose particles. It is shown that the method is a generaliz-ation of the Holstein-Primakoff transformation of angular momentum com-ponents.

Inelastic Neutron Scattering in the Superconducting and Normal Phases of Ta

(S. M. Shapiro and O. W. Dietrich)

Room temperature phonon dispersion curves of several transition metals reveal interesting anomalies which require more than the ordinary

Born-von Karman force constant analysis to fit the observed data. It has been suggested that these anomalies are intimately related to the super-conductivity properties of the transition metals[25]. Recently, inelastic neutron scattering experiments on Nb showed changes in the peak position and line width of several small q transverse phonons when Nb became superconducting below T_c = 9.2 K[26]. The room temperature dispersion curves of Ta also show some anomalies and Ta becomes superconducting below T_c = 4.4 K. High-resolution studies of the transverse phonons propagating along (001) and (110) directions with polarization along (010) and $(1\bar{1}0)$ respectively, have been performed down to a temperature of 4.5 K, just above T_c. The peak positions of several (001)-T phonons do not decrease with temperature as observed in Nb, but show a slight in-crease ($\langle 1\%$) in frequency on cooling. The (011)-T_1 modes also show a slight increase on cooling. Experiments are underway to investigate further the phonon behaviour in the superconducting phase.

Phase Transition in Deuterated CsDA

(R. A. Cowley, O. W. Dietrich, and S. M. Shapiro)

Caesium dihydrogen arsenate exhibits a ferroelectric-structural phase transition like the much studied transition in potassium dihydrogen phosphate (KDP). The neutron scattering investigations of KDP a few years ago at Chalk River and Brookhaven showed critical neutron scattering associated with the phase transition, but it was not possible to observe any inelasticity of the critical scattering. This indicates that the critical fluctuations in KDP are slow compared to the typical neutron interaction time of 10^{-12} s. There were reasons to believe that if critical fluctuations occurred in CsDA they would relax faster. The inelasticity might then be observed with neu-tron scattering.

We found that deuterated CsDA undergoes the phase transition at 205 K. However, an extensive search above this temperature round many Bragg reflections revealed no observable signs of critical scattering. This led us to conclude that the transition is "too much" first order for critical fluctu-ations to occur.

[25] H. G. Smith, Superconductivity in d- and f-Band Metals, (D. H. Douglass, Editor), AIP Conference Proceedings No. 4, New York, 321 (1972)

[26] G. Shirane, J. D. Axe, and S. M. Shapiro, Solid State Commun. (to be published)

Above the phase transition the crystal structure is tetragonal, but it changes to orthorhombic below the transition. This causes a domain structure to occur in the a-a planes. At the same time satellites show up around Bragg reflections (hkℓ) of non-zero ℓ-values. We have observed two non-commensurate sets of side peaks, each of them with higher harmonics. At present we do not know the origin of the periodic structure which gives rise to these satellites and further investigations are planned.

Phonons in C_2F_6

(O. W. Dietrich, B. M. Powell, and E. Warming)

In the temperature range 104-172 K, C_2F_6 exhibits a plastic phase, which is thought to be due to a free rotation of the F ion around the molecular axis. A study has been undertaken to measure the rotational mode by neutron scattering. A single crystal has been grown, and preliminary measurements in a few symmetry directions have revealed a broad overdamped rotational band.

The Nematic to Isotropic Phase Transition in the Liquid Crystal PAA

(T. Riste (IFA, Kjeller, Norway) and H. Bjerrum Møller)

The liquid crystal PAA exhibits a transition from a nematic phase, which is a liquid state with orientational order of the molecular axis of the elongated molecules, to an isotropic liquid state in which this order is zero. A coherent elastic neutron diffraction investigation of this transition and its dependence on applied magnetic field was initiated. The magnetic field aligns the molecules in the nematic phase and therefore changes the intensity of the peaks in the structure factor $S(\varkappa)$. The intensity of the liquid peak at $\varkappa = 1.8$ Å^{-1} is thus increased by application of a magnetic field perperdicular to the scattering vector.

In addition the intensity at $\varkappa = 1.8$ Å^{-1} shows two peaks as a function of temperature in the region of the nematic to isotropic transition, separated by approximately 1 K. The intensity of these peaks decreases on application of a magnetic field both perpendicular to and in the direction of the scattering vector, and they disappear entirely at about 10 mT. These two peaks are interpreted as critical scattering associated with the stability limits of the nematic and isotropic phases respectively.

Structure of Amorphous D_2O Ice

(J. Wenzel, C. U. Linderstrøm-Lang (Chemistry Department), and S. A. Rice (University of Chicago))

We have recently completed a neutron diffraction study of amorphous D_2O ice in order to determine its structure. One motivation for this research is to verify that amorphous ice is a suitable model for liquid water, which may be studied at low temperatures where the effects of structure and molecular motion can be separated best. Therefore, the co-ordination sphere model of water is being extended to two co-ordination spheres, in order to account for the longer range of order in amorphous ice.

A second reason for the study of amorphous ice is that it is a new but "typical" glass, in which the tetrahedral co-ordination is a consequence of the hydrogen bonding properties of the water molecule. A structural study of amorphous ice will offer further evidence in support of one of the two rival theories of glass structure, either the microcrystalline theory or the random network theory. Results of model calculations indicate that the neutron diffraction measurements disagree with the scattering calculated using the microcrystallite hypothesis. Work is in progress to develop a random network model which may be compared with the scattering data.

Experimentally, the amorphous ice was studied using a 2-axis spectrometer over a wide range of momentum transfers (0.5 Å^{-1} $< \varkappa <$ 13 Å^{-1}), with unusually good signal-to-background ratios (typically 30:1), with high statistical accuracy (better than 1%), and with small sample size (0.5 g).

For amorphous structure determination the uncertainty in the data corrections limits the accuracy of the results. We determined that the published Placzek correction for water (using an effective mass of 20/3) does not work well for amorphous ice. Changing the effective mass to about 4 gives a much better fit to the theoretical scattering at large $\varkappa$. By Monte Carlo simulation, we tested that the usual assumption of an isotropic multiple scattering correction is justified. Other data corrections included an absorption correction and a calibration experiment in which the geometric constant of the spectrometer was determined from the scattering of a vanadium standard.

The fundamental measure of the structure, the structure factor $S(\underline{\varkappa})$, was determined from the experimental data by applying the above corrections and subtracting the incoherent portion of the scattering. This is shown in fig. 11. $S(\underline{\varkappa})$ is being compared with calculations of the structure factor based on models and has been Fourier-transformed to yield the radial distribution function of amorphous D_2O ice.

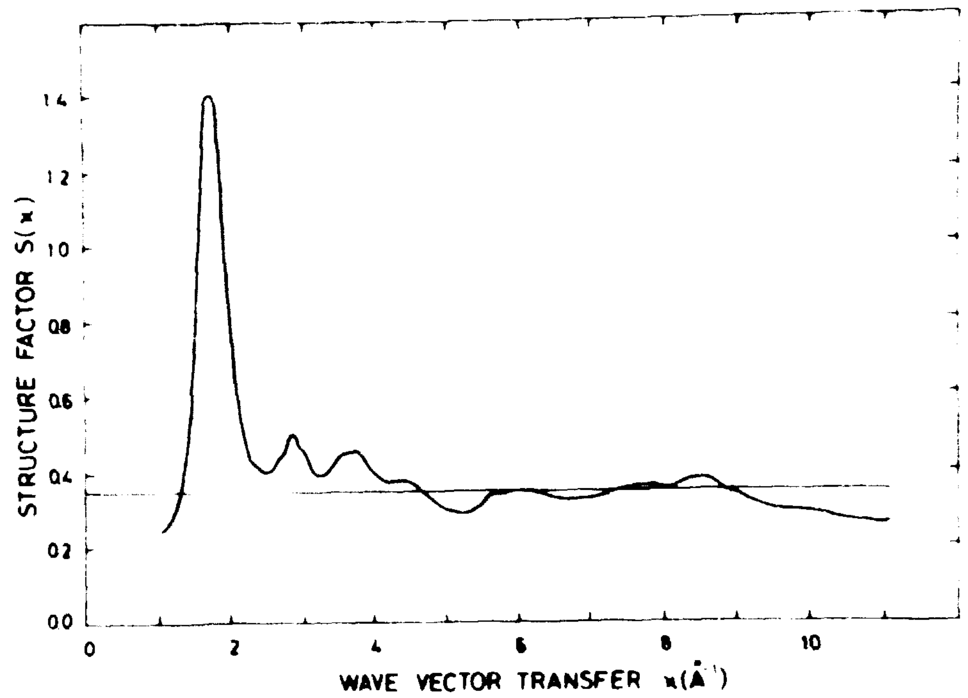

Fig. 11. The structure factor S(κ) of amorphous D_2O ice. All data corrections have been made, the scattering has been normalized using a vanadium standard, and the incoherent portion of the scattering has been subtracted. The horizontal line represents the asymptotic value of the structure factor.

Further work towards preparation of other novel amorphous materials is underway. It will include trial compounds such as the rare gases, quasi-spherical molecule compounds, and hydrogen-bonded systems.

Neutron Scattering from Amorphous Se

(F. Y. Hansen (Technical University of Denmark), K. Carneiro, and J. W. Wilkins (Cornell University))

Neutron scattering in amorphous Se at various temperatures was initiated for two reasons. Firstly, there has been some controversy concerning the structure of this material, secondly, the dynamics of amorphous systems is at present a subject of intense discussions.

In fig. 12 we show the structure factor $S(\underline{\kappa})$ at room temperature determined by neutron diffraction. This result was obtained after correcting for background, absorption, incoherent scattering, multiple scattering, and inelastic scattering through the Placzek corrections. In order to minimize these corrections measurements were made at wavelengths between 0.852 Å and 2.365 Å. To make the final results as reliable as possible, we also used the analytical properties of the pair distribution function g(r) which is

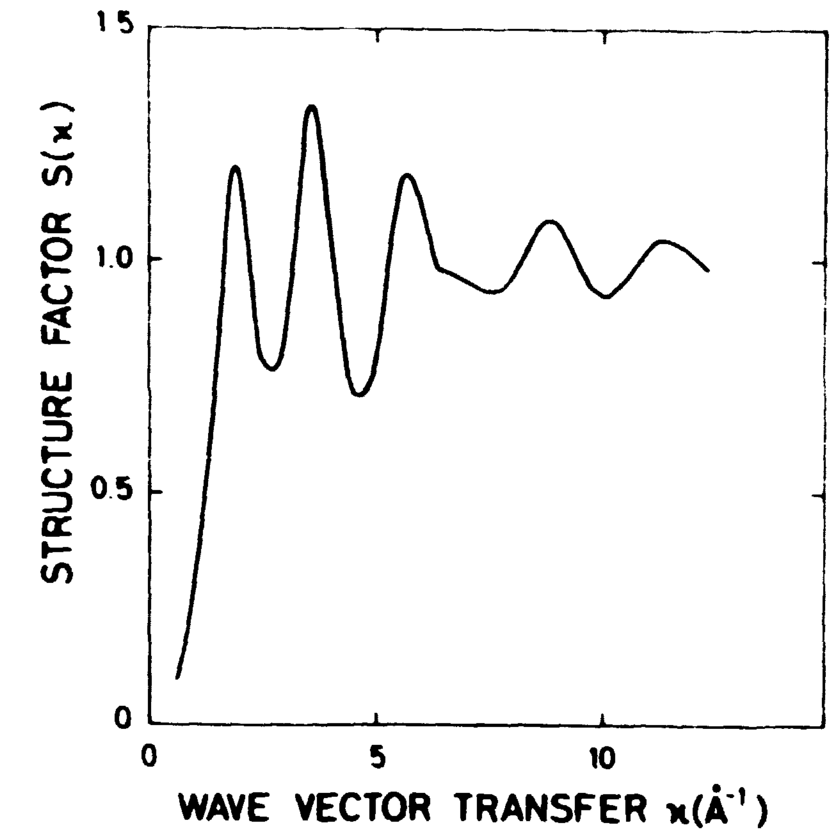

Fig. 12. The structure factor for amorphous Se obtained by neutron diffraction, after final corrections. The dashed line represents the asymptotic value of the structure factor at large κ.

related to $S(\underline{\kappa})$ through

$$g(r) = 1 + \frac{1}{2\pi^2 \rho_0} \int_0^\infty \kappa \{S(\kappa) - 1\} \sin(\kappa r) d\kappa.$$

The dynamical properties of amorphous systems are of interest partly because it is not clear how the disorder influences the general dynamical properties as compared to phonons in crystals. Further, the recently found specific heat anomaly in glasses might be caused by population of excitations which may be observed by neutron scattering. We have observed that the elastic scattering, $S(\kappa, \omega \sim 0)$, (i. e. the extension of the Rayleigh line) has a natural energy width which is significantly less than that required to explain the specific heat anomaly. The other possibility that the phonons at low wave vectors show a significant natural width is now being considered theoretically and experimentally.

Neutron Scattering in Liquid N_2

(J. P. McTague (University of California, Los Angeles) and K. Carneiro)

Coherent inelastic neutron scattering was performed on the classical, homonuclear, diatomic liquid, N_2. The scattering can be expressed as a sum of scattering from partial waves, each of which has different wave vector dependent form factors. This allows a separation of the partial waves.

In the case of liquid N_2 the results are as follows. For wave vectors $\varkappa \lesssim 2.4$ Å^{-1} the scattering is dominated by the centre of mass motion (s-wave), whereas at $\varkappa \sim 5.5$ Å^{-1} only the tensorial rotational relaxation (d-wave) contributes to the scattering. Preliminary results are displayed in fig. 13. At very small wave vectors $\varkappa \sim 0.1$ Å^{-1} (insert A), the remnant of the sound wave is seen both by "extended hydrodynamics", and by computer simulation. Extended hydrodynamics is a theory for viscous fluids taking shear viscosity into account. It should be stressed that ordinary hydrodynamic theory for a viscous fluid yields that the sound wave is overdamped at this wave vector. It is to our knowledge the first experimental study of this phenomenon in a classical liquid.

For intermediate wave vectors (inserts B and C) the line shapes show no clear propagating modes. However, if compared to similar results for liquid argon, the ω-dependence of $S(\varkappa, \omega)$ is different in the two liquids. This is a direct indication of coupling between rotational and translational modes. Finally we show in insert D the line shape observed from pure d-wave scattering.

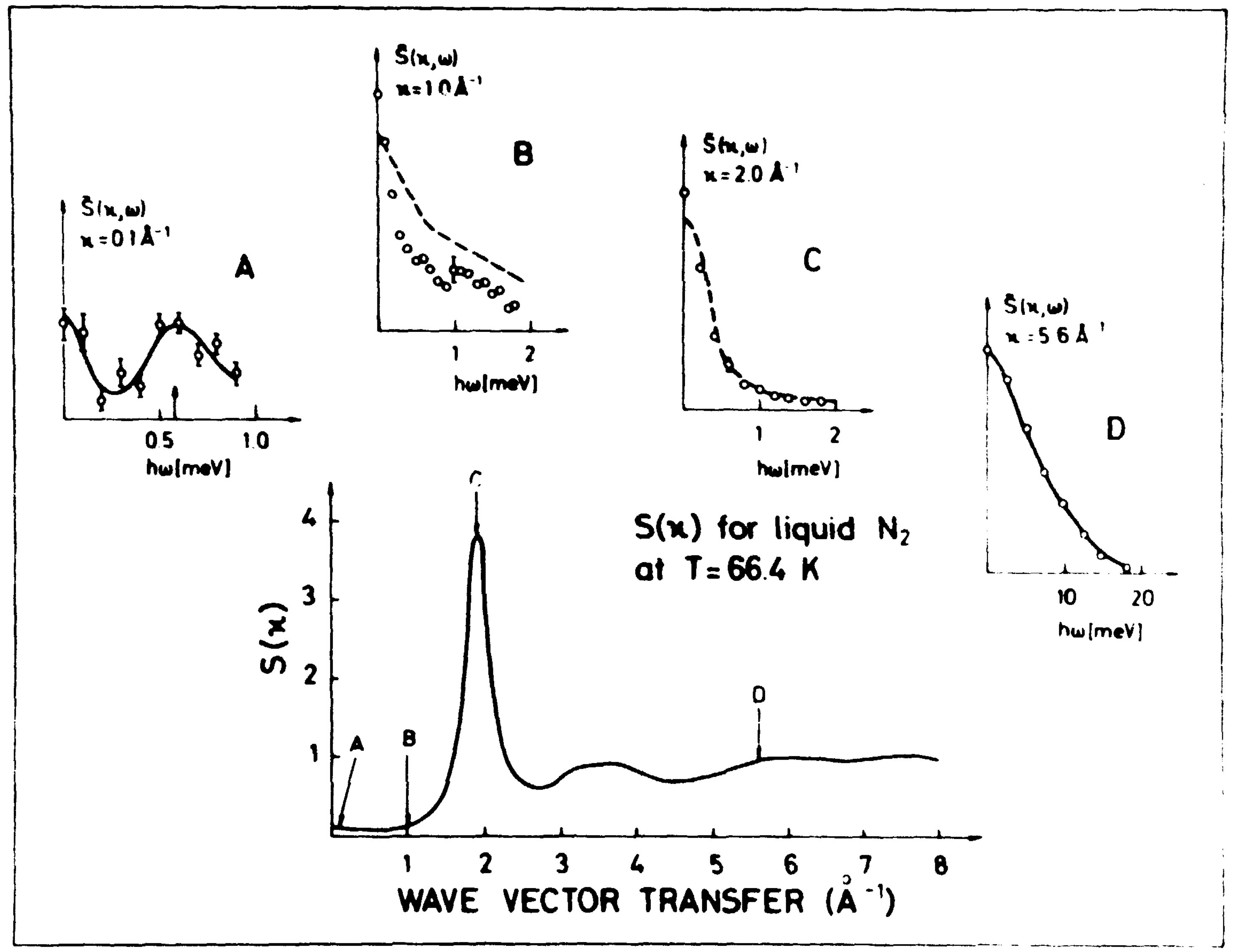

Fig. 13. Neutron scattering from liquid-N_2. The symmetrized, classical scattering law $\tilde{S}(\varkappa, \omega)$ is shown at the characteristic points of the structure factor $S(\varkappa)$. o are experimental points with typical error bars indicated. Full lines are guides for the eye. Dashed lines are similar results for liquid-A. In insert A the arrow indicates the extrapolated position of the ordinary sound wave.

Neutron Scattering from Solids or Liquids under Moderately High Pressures

(K. Carneiro, M. Nielsen, and W. Kofoed)

The construction of the equipment for neutron scattering on samples at liquid-helium temperatures and hydrostatic pressure up to 6 kbar was finished and the first sample container made for 2 kbar, is now in operation. The pressure and temperature dependence of the structures and the dynamics of solid D_2 and H_2 are under investigation, with particular attention to the proposed structural phase transition from hcp to fcc.

Structure Studies under High Pressure

(B. Buras, B. Lebech, W. Kofoed, and G. Bäckström (University of Umeå, Sweden))

A high-pressure cell for neutron diffraction studies of powdered samples has been constructed and tested up to about 35 kbar. The cell is similar to that used by Brugger et al.[27]. It consists of a housing made of an aluminium oxide cylinder, 6.3 cm high by 3.2 cm in diameter with a 0.63 cm bore. The cell is supported by hardened steel wedges and these are supported by a binding ring. The steel wedges are 30° segments of a cylinder, such that there are 0.34 cm wide gaps every 30°. There are also number of similar gaps (2.4 cm high) in the supporting binding ring permitting the use of scattering angles of 30°, 60°, 90°, and 120°. Tungsten carbide pistons transmit to the sample the force from two 30 ton rams driven by an oil press. The pressure was calibrated by utilizing the pronounced changes in the electrical resistivity of Ce and Bi when passing through the phase transitions.

Two methods of fixed scattering angle diffraction have been tested in conjunction with the high pressure cell. In one method - the monochromator scan method (MS) - a monochromatic neutron beam of varying neutron wavelength is scattered through one of the available angles by the powdered sample and the intensity of the scattered neutrons is then measured as a function of the incident neutron wavelength. The monochromator-analyser scan method (MAS) is an obvious extension of (MS). The scattered neutrons are reflected from a single crystal analyser set to reflect neutrons which are elastically scattered by the sample. As expected, the use of an analyser crystal improves the peak to background ratio.

For the tests we used a 3-axis spectrometer with a variable incident wavelength and studied samples of KNO_3 and Bi. The phase transitions at room temperature of KNO_3 II to KNO_3 IV (at 3 kbar), Bi I to Bi II (at 25.3 kbar), and Bi II to Bi III (at 26.8 kbar) were observed (fig. 14).

27) R. M. Brugger, R. B. Bennion, T. G. Worlton, and E. R. Petersen, Research Applications of Nuclear Pulsed Systems. Proceedings of a Panel held in Dubna, July 1966 (IAEA, Vienna, 1967) 35

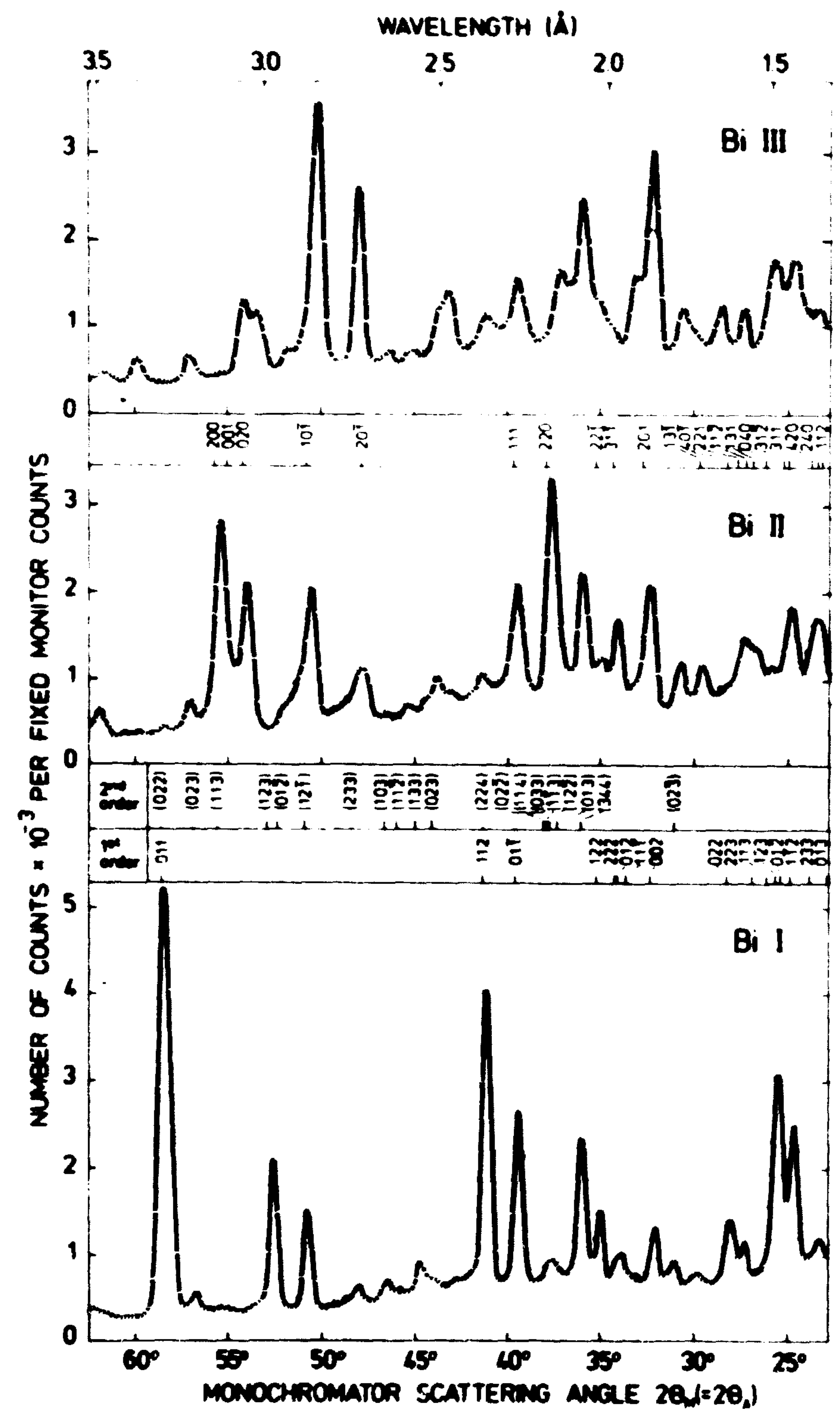

Fig. 14. Neutron diffraction patterns of Bi I at atmospheric pressure, Bi II at 26 kbar and Bi III at 30 kbar, obtained by means of the MAS method using pyrolytic graphite as both monochromator and analyser. The scattering angle equals 60°.

Neutron Slowing-Down by Bragg Reflection from a Moving Single Crystal

(B. Buras, K. Carneiro and S. E. Nielsen, E. Præstgaard (Chemical Laboratory III, University of Copenhagen), and S. Steenstrup (Physical Laboratory II, University of Copenhagen))

Previous experiments have shown[28] that thermal neutrons can be slowed down by Bragg reflection from a moving single crystal. Further neutron diffraction experiments were carried out and compared to analytical calculations and simulation experiments by means of the Monte Carlo technique. To simplify the calculations it was assumed that the moving mosaic crystal is infinitely long in the direction of movement and that the reflectivity is 1. With these assumptions the number of reflected neutrons and the distributions of velocity vectors were calculated. It was shown that the root mean square deviation (RMS) of the velocity distributions increases as the ratio of the velocities of the incident neutrons to the reflected neutrons. The RMS of the polar angle distribution of the reflected neutrons is never larger than the mosaic spread of the moving crystal regardless of the divergence of the incident beam. This was verified experimentially. The RMS of the azimuthal angle and the solid angle extended by the reflected neutrons are increased in the slowing-down process. However, the cold neutron flux per unit wavelength and unit solid angle can be larger than the cold neutron flux obtained directly from the incident Maxwellian spectrum.

2. PLASMA PHYSICS

Solid H_2 Film

(H. Sørensen)

The interaction between a fusion plasma and a pellet of solid H_2 is the sum of many different interactions. To study some of these interactions an experimental arrangement has been designed and constructed (fig. 15). The arrangement consists of a central vacuum chamber of ultra-high vacuum quality (~10^{-8} torr) with several port holes (37 mm diameter). A solid H_2 target placed in the centre of the chamber can be bombarded by particles of energies in the keV range. The interactions are then studied either through other port holes or by means of equipment placed inside the vacuum chamber. The incident particles may come from an electron gun (up to 3 keV) or a duoplasmatron ion source (up to 10 keV).

[28] B. Buras, J. Kjems, and K. Carneiro, Risø Report No. 288, 35 (1973)

The target layer of solid H_2 is made by letting a molecular beam of H_2 impinge and solidify on a cooled quartz crystal. It is possible to make films of H_2 at 3.0 K and D_2 at 4.2 K. The film growing technique was tested in two earlier experimental arrangements. With an improved system that fits into the central vacuum chamber it is possible to grow a film of 50μ thickness in 10 minutes. The quartz crystal can be heated and the film can then be removed again in 1-2 minutes. The quartz crystal acts as a micro-weight and it is therefore useful for a study of the film growing technique. The sensitivity of the quartz crystal is such that a 10 Å layer of D_2 gives a frequency change of 1 c/s at a resonance frequency of 5 Mc/s. By looking through holes in the thermal radiation shields we saw that the films were limpid and transparent. Polarized light did not reveal any crystalline structure. Later, when the film growing technique is known, a less difficult substrate can be used.

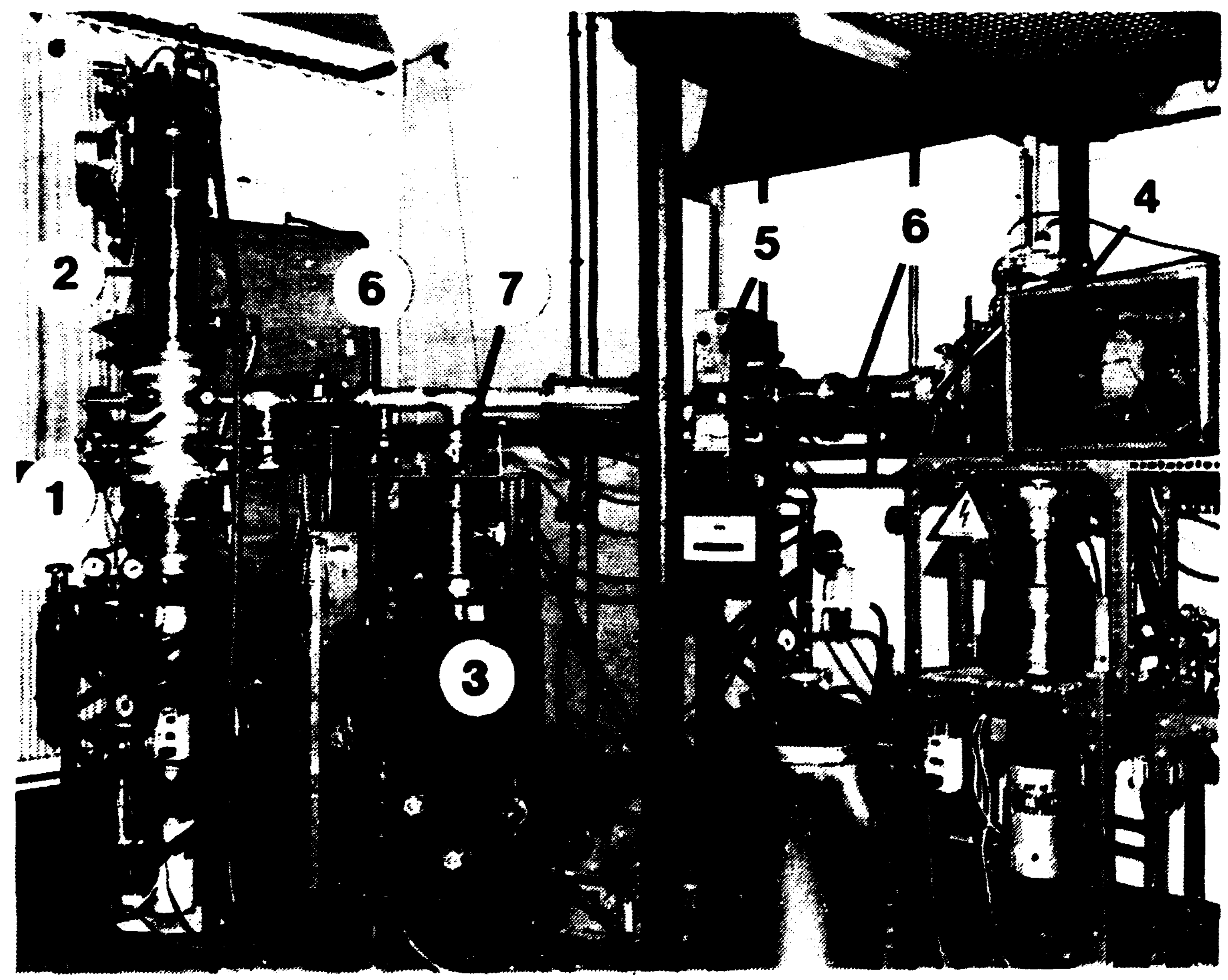

Fig. 15. The arrangement for work with solid H_2 films. (1) Central vacuumchamber. (2) Cryostat. (3) System for control of the vapour pressure of the liquid-He. (4) Duoplasmatron ion source. (5) Analysing magnet. (6) Beamtube. (7) Pumping system for differential pumping.

To study interaction processes in a film of solid H_2 bombarded by charged particles is experimentally more difficult than similar studies of other solids. The solid H_2 film must be made and kept at liquid He temperatures behind shields protecting against thermal radiation. It may also be necessary to work with pulsed beams since solid H_2 is an electric insulator which charges up quickly upon bombardment with charged particles.

The first irradiations of a film will take place soon, and the future work will then be directed towards developing suitable methods for the study of interactions.

Pellet - Rotating Plasma Interaction

(L. W. Jørgensen, A. H. Sillesen, and F. Øster)

In order to improve the lauching part of our solid H_2 pellet launcher we have changed the thermal joints. In addition, careful control of the surface smoothness of the joints, the background pressure, and the pressure on the operating pistons ensures a reasonable reliability.

The pellet mass loss was then measured versus the energy of the plasma. To determine the energy we used a diamagnetic loop. Hereby the total energy input to the pellet is recorded, but the measured energy is integrated over the cross section of the puffatron. The mass loss is proportional to the energy input, in contrast to the dependence between the loss and the electric field squared. A possible explanation is that the lifetime of the high-energy phase varies for different rotational energies of the plasma.

The measured loss is higher than expected. It was suggested[29] that the shielding neutral gas layer formed around the pellet is destroyed by the charge exchange process $H^+ + H_2 \rightarrow H + H_2^+$. To verify this, the loss was also measured in a He plasma, in which the loss was expected to be considerably smaller. No significant difference in loss in the two kinds of plasmas was detected. The discrepancy between the measured and the calculated mass loss in the pellet - plasma interaction is reduced by taking into account the actual trajectories of the ions in a rotating plasma. A theory, based on a single-particle picture, predicts an energy input which is about a factor of two higher than that predicted by the simplest fluid theory.

A possible disintegration and the apparent deflection of the pellet caused by the interaction might be observed in two consecutive discharges with a time delay of a few mseconds. We tried to observe the pellet in the second discharge by opening the image converter camera twice. The observation failed, possibly owing to a disintegration of the pellet, but more likely owing to a lack of illumination in the second discharge.

[29] C. T. Chang, A. H. Sillesen, H. Sorensen, and F. Øster, Risø Report No. 288, 38 (1973)

Previously, we measured the initial ion energy spectrum of the puffatron plasma by means of a neutral particle detector. This detector has been calibrated using CO_2 as a stripping gas for energies in excess of 800 eV, and is now used to measure the neutral flux in pellet - plasma interaction. The pellet acts as a neutral particle source in an otherwise fully ionized plasma. These measurements may therefore give a space and time resolved determination of the energy imparted to the pellet by the ions. As expected, preliminary results show that high-energy neutrals are detected for a longer period in the interaction case.

Pellet Refuelling Problem - Theoretical Aspects

(C. T. Chang)

An order of magnitude estimate based on the concept of stopping power and range showed that for a reactor at 20 keV, the initial phase corresponding to the direct impact on the pellet of energetic particles from the fusion plasma lasts less than 10 ns. Since this is much shorter than the pellet penetration time ($\sim$0.1 ms), the disintegration of the pellet will be governed mainly by the expansion of the cold ablated plasma cloud against the magnetic field. The initial ablation rate as well as the charge of the pellet, however, is governed by the direct impact phase.

A re-examination of Rose's magnetic shielding model[30] revealed that for the shielding mechanism to work, the operating range of β is limited. For a 5 GW reactor operating at 20 keV with a confinement field of 4 T, one has $0.16 < \beta < 0.18$ for a pellet of radius 7.5 mm. The β-value is higher than desired. A refinement of the model and investigation of other possible shielding mechanisms are therefore needed.

Magnetically Driven Shock

(C. T. Chang)

A theoretical study of the distance between the shock and the current sheet was made by taking effects such as ionization, finite conductivity, and viscous boundary layer into account. None of these effects offers a

[30] D. I. Rose, Culham Laboratory Technology Division Memorandum No. 82 (1968)

satisfactory explanation of the small separation observed at low discharge pressures. This is probably due to the fact that the driving current is distributed in a growing layer and not confined within a thin sheet. We must therefore conclude that the shock is formed within the current sheet itself in contrast to the usual concept that the shock is formed ahead of the current sheet.

To clarify the formation mechanism and develop a diagnostic technique for possible future study of the plasma - solid interaction, work to determine the plasma refractivity from differential interferograms was initiated. To supplement this, an estimate of the refractivity due to the electron component was made from time-elapsed holographic interferograms.

Study of Ion Acoustic Waves through Green's Functions

(H. C. S. Hsuan (University of Iowa, U. S. A.) and V. O. Jensen)

A theoretical study of the propagation properties of ion acoustic waves in collisionless streaming plasmas has been undertaken. The results show that in general the wave will damp algebraically rather than exponentially with distance from the exciter.

Absolute and Convective Ion Beam Instability Studied through Green's Functions

(V. O. Jensen, P. Michelsen, and H. C. S. Hsuan (University of Iowa, U. S. A.))

In the Q-machine plasma it is possible to obtain a double-humped ion velocity distribution function by utilizing charge exchange processes. With this distribution function and with an electron to ion temperature ratio increased to at least 3.5 times the ion temperature, the plasma becomes unstable to the ion beam instability.

A theoretical study of this was performed using the Vlasov equation for the ions and assuming the electrons to behave as an isothermal fluid. The response to an initial perturbation of the form of a δ-function in space can be divided into two parts: a self-similar, damped part of the form $t^{-1} \cdot h(x/t)$ and an unstable exponentially growing part. Depending on the form of the ion velocity distribution in the initial perturbation, the self-similar part will be the dominant one for a shorter or longer time. Therefore it should be possible in an experiment to observe this part independently of the growing one. It turns out that the instability will be absolute in some frames of reference, but normally it will be observed as a convective one in an experiment.

To study the instability experimentally it is necessary to heat the electrons, which can be done by using the electron cyclotron resonance. Microwave equipment has been ordered for this purpose.

Collisionless Damping

(V. O. Jensen and P. I. Petersen)

Exact theoretical treatments show that the damping of ion acoustic waves in collisionless plasmas does not vanish when the derivative of the undisturbed distribution function at the phase velocity equals zero.

Calculations of Propagation of Linear Density Perturbations in Collisionless Plasmas

(L. W. Jørgensen and H. L. Pécseli)

Analytic calculations are performed using the full set of linearized one-dimensional Vlasov equations for electrons and ions coupled through the Poisson equation. Two initial perturbations are considered: a step-like and a pulse-like density perturbation. A comparison of these results with published experimental results and non-linear calculations indicates that results obtained by a linear calculation can be used as an approximation in non-linear problems in a stable plasma, even for high electron to ion temperature ratios, ($T_e/T_i \simeq 25$).

Investigation of Plasma Instabilities in the Q-Machine

(N. D'Angelo, H. L. Pécseli, and P. I. Petersen)

Spectral measurements were performed of ion acoustic turbulence excited in the Cs plasma of a Q-device, modified to a magnetic cusp geometry. The frequency power spectra $F(f) \propto f^{-3}$ have been measured. An interpretation is proposed in terms of a $1/k^3$ spectrum, and the turbulence clearly reflects the driving source ($\nabla B \times B$ electron drift).

Investigation of the Farley instability in the Q-machine has been started. In this case the plasma is created by surface ionization on a 2-mm-thick wire shaped as a spiral. Hereby a radial electric field is created that causes the plasma to rotate as a solid column. At a background pressure of $\sim 1\text{-}1 \times 10^{-2}$ mm Hg the ion neutral collision frequency is equal to the ion cyclotron frequency, while the electron neutral collision frequency is much smaller than the electron cyclotron frequency. This causes the electrons to drift through the ions and gives rise to the Farley instability.

Non-linear Wave Coupling between Electromagnetic and Ion Acoustic Waves

(P. Michelsen (work performed during a visit to Yale University, U.S.A.))

A non-linear wave coupling experiment was performed in an electron beam generated plasma. The plasma was flowing through a cylindrical microwave cavity in which an amplitude modulated transverse magnetic wave was excited. The electrons oscillate in the microwave field and owing to the modulation an ion acoustic wave can be excited with a frequency equal to the modulation frequency. The amplitude of this wave was measured with a grid-shielded collector. The result was found to be in reasonable agreement with a calculation of the coupling coefficient based on the Vlasov equation, when the ion neutral collisions were taken into account.

Linear Plasma Oscillations Described by a Superposition of Normal Modes

(H. L. Pécseli)

The effect of ion motion is introduced in van Kampen's treatment of electron oscillations. It is demonstrated that ion acoustic waves excited by absorbing grids in a single-ended Q-machine can be described as superposition of van Kampen modes although the problem now is a boundary value problem instead of an initial value problem. This solution suggests a simple mathematical description of the so-called "pseudo waves".

Electron Heating in a Single-ended Q-Machine

(H. L. Pécseli and P. I. Petersen)

In order to increase the effect of collective interaction an increase in the electron ion temperature ratio is desirable. Using microwave power of the order 150 mW at the electron cyclotron frequency, it is possible to increase the electron temperature by a factor of 2-3 without disturbing the ions and without a serious increase in the noise level. By introducing a current along the field lines turbulent heating is obtained, but in this case the ion velocity distribution is severely altered and the noise level is increased.

3. NUCLEAR PHYSICS

An attempt to Form the ^{236}U Fission Isomer with Thermal Neutrons

(V. Andersen and C. J. Christensen)

An experiment to study fission isomers is being designed at the DR 3 reactor. A ^{235}U target is irradiated in a thermal neutron beam. Delayed coincidences between simultaneous internal conversion electrons and U-X_L-rays and delayed fission fragments are detected. The main feature of the detector geometry is shown in fig. 16A. A 4π solid angle for electrons and

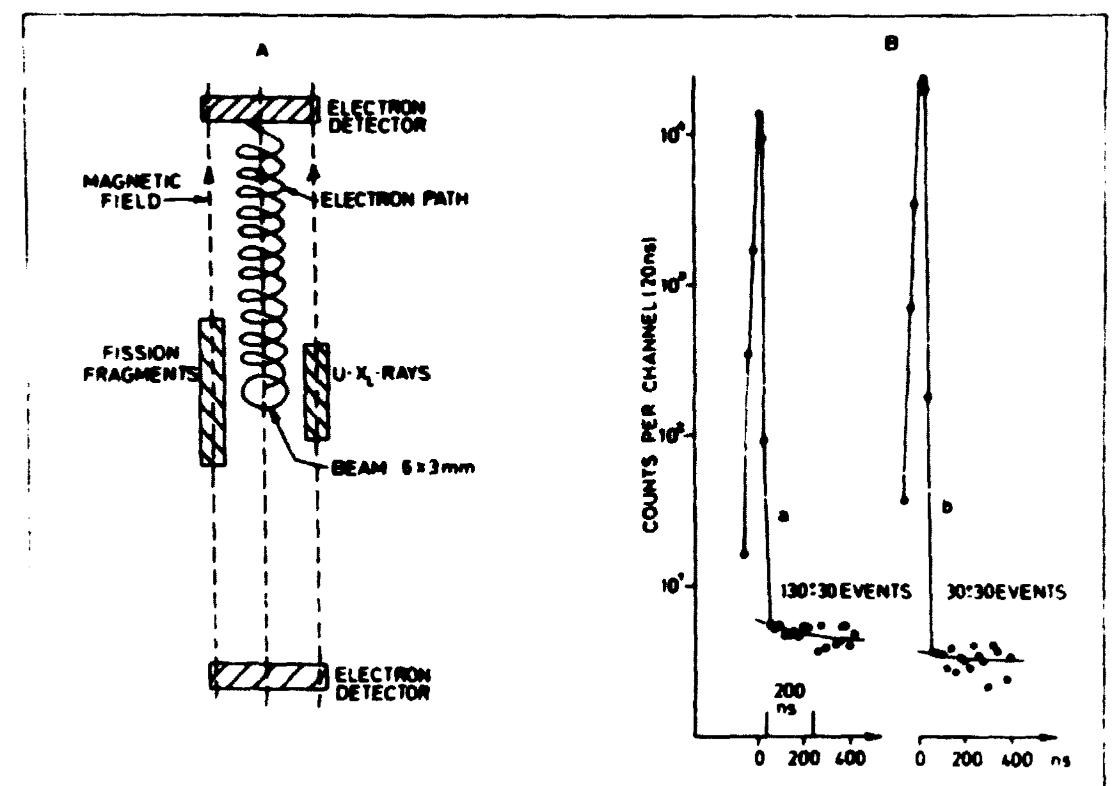

Fig. 16. A) Schematic of target and detector geometry. A homogeneous magnetic guide field of 0.7 T secures a 4π electron solid angle. Therefore $\epsilon_1 = 1$, $\epsilon_F = 0.6$, $\epsilon_x = 0.15 \times (U\text{-}X_L)$.
B) Delayed coincidence spectrum: Fragments delayed after prompt e-x coincidence for electron energies 15-300 keV. Curve a) for U-X_L-rays (12.7 - 14.5 keV ($L\alpha$) plus 16.3 - 18.1 keV ($L\beta$)) shows the fission isomer shoulder. Curve b) (14.5 < E_x < 16.3 keV (i.e. fragment X_k-rays)) shows the absence of instrumental effects. A least-squares fit of an ~100 ns half-life on top of accidental background gives 130 ± 30 events in a), 30 ± 30 events in b), showing the sensitivity of the method.

a close geometry of fragment and X-ray detectors yield high efficiency for triple coincidences. The detection of characteristic U-X_L-rays plus electrons, rather than just γ-rays, yields good selectivity for pre-fission electromagnetic transitions. A five-parameter pulse height analyser system with event-by-event magnetic type storage will be used for unscrambling the correlation between electron energies and fragment delay time.

Preliminary measurements of the fragment time-delay spectrum seem to show that we shall be able to see isomer to prompt fission ratios lower than 10^{-5}. This is more than a factor of two better than the lowest upper limit hitherto reported. Fig. 16 B shows the time spectrum observed. The spectrum indicates a statistically significant isomer formation with a value of 10^{-5} for the above-mentioned ratio. More measurements to improve statistics, and studies of the accompanying electron spectra are needed and have been started.

4. METEOROLOGY

Wind Profiles at Risø

(N. O. Jensen, E. L. Petersen, and E. W. Peterson)

Analysis of data from Risø's 120 m tower reveals that for certain wind directions distinct kinks appear in the vertical profiles of the horizontal mean wind. The kinks in the profiles which for some wind directions are double kinks, are believed to relate to changes in the roughness of the upstream terrain[31, 32].

A more recent investigation[33] of neutral wind profiles concludes that the use of gradient Richardson numbers biases the wind profiles, selected for the neutral case, towards higher than average friction velocities and roughness lengths. Furthermore there are indications of a temperature anomaly in the Risø temperature profiles of about 0.4^{o} C per 100 m for the years 1963-1971. The doule kinks in some of the profiles as selected by Panofsky and Petersen[31] may not be caused by nearby terrain features

31) H. A. Panofsky and E. L. Petersen, Quart. J. Roy. Meteorol. Soc. 98, 845 (1972)

32) E. L. Petersen and P. A. Taylor, Quart. J. Roy. Meteorol. Soc. 99, 329 (1973)

33) E. W. Petersen, submitted to Quart. J. Roy. Meteorol., (1973)

but by some, as yet undetermined, mesoscale effect. The logarithmic wind profile law for neutral profiles in the surface layer does not appear valid for heights above 100 m. The analysis is being continued. In the future, the stable and unstable cases will be studied in more detail with emphasis on mesoscale influences on the shapes of the wind and temperature profiles.

Turbulence in the Atmospheric Surface Boundary Layer

(N. E. Busch, S. E. Larsen, and N. W. Nielsen)

The turbulent diffusivities K_h and K_m for the vertical exchange of sensible heat and momentum are often assumed to vary according to a mixing length hypothesis: $K \approx \ell V$, where ℓ and V are length and velocity scales respectively, associated with the turbulence.

On the basis of data obtained during the Kansas 1968 experiment, it is found that the most important length scales are $\lambda_{m\alpha\beta}$, $(\alpha, \beta = u, v, w, T)$, where $\lambda_{m\alpha\beta}$ is the wavelength corresponding to the frequency at which the logarithmic co-spectrum $nS_{\alpha\beta}(n)$ has its maximum.

Analysis of profile data obtained simultaneously with the turbulence data shows that the flux-profile relationships are well described over a wide stability range by

$$K_m = c_m \cdot \lambda_{muw} \cdot u \qquad \text{and} \qquad K_h = c_h \cdot \lambda_{muu} \cdot u_* ,$$

where u_* is the friction velocity, and $c_m \simeq c_h \simeq 15$ are "universal" constants.

Analysis of spectra, wind profiles, and temperature profiles shows that in hydrostatically stable and in near neutral conditions, the surface boundary layer obeys Monin-Obukhov similarity laws reasonably well. In moderately to strongly unstable conditions (local free convection), however, the data clearly indicate deviations from M-O similarity. It is suggested that the deviations are due to pressure forces associated with plume/eddy activity. The data appear to support this suggestion, which leads to a reformulation of the definition of "local free convection" based on the total energy equation for the flow.

Numerical Modelling of the Wind Structure in the Planetary Boundary Layer

(N. E. Busch and N. O. Jensen)

The daily variations of wind speeds, wind directions, and temperatures at Risø exhibit characteristics which in general are consistent with those found in other places over quite different terrain. However, in many

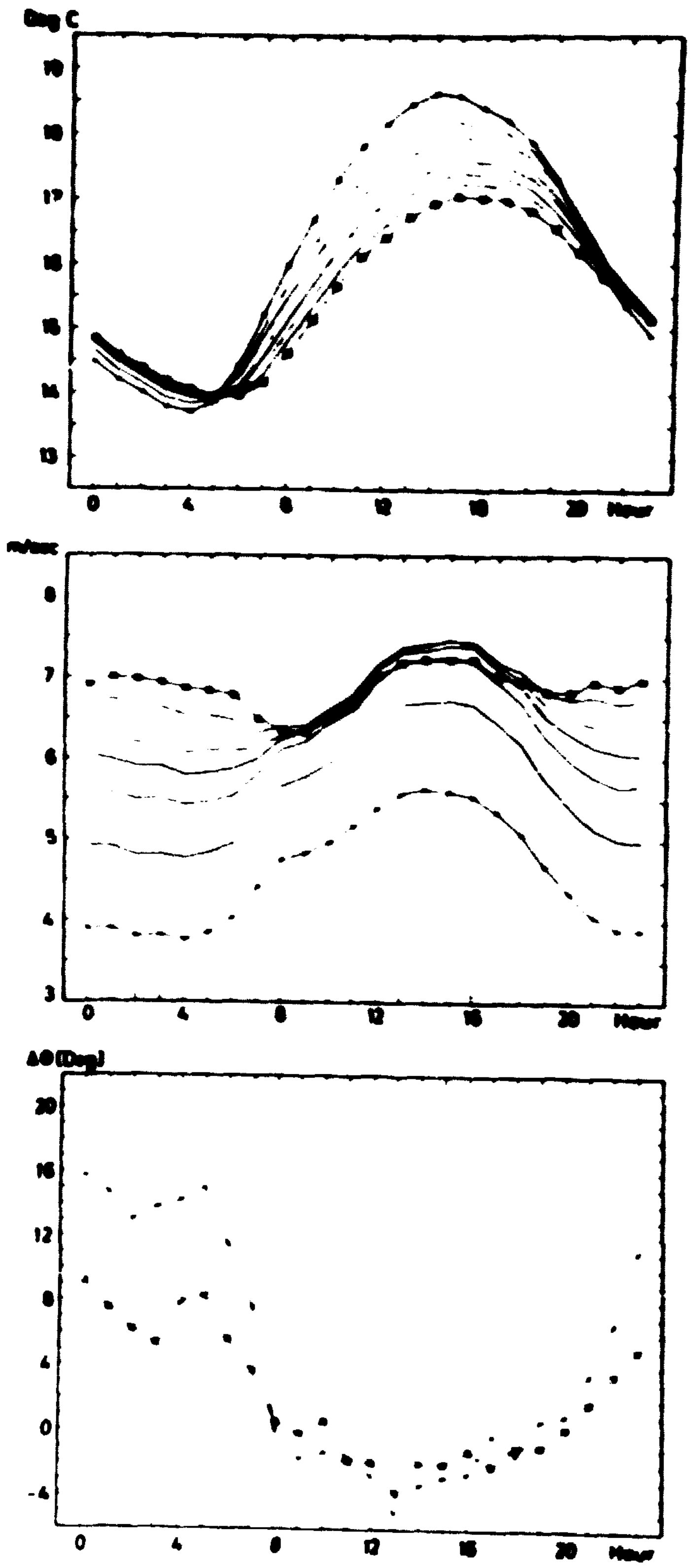

Fig. 17. The upper graph shows the variation of temperature with time of the day at different heights: 2, 7, 23, 39, 56, 72, 96, and 123 m. The 2 m height is indicated by ■-■ and 123 m by ●-●.

The middle graph displays the variation of wind speeds measured at the same heights except that wind speeds were not measured at 2 m, so that 7 m is indicated by ■-■.

The bottom graph: ■-■ represents the angle between the wind directions at 123 m and 7 m; ●-● gives the angle between the directions at 56 m and 7 m. Angles are positive if the wind direction is turning clockwise with height.

The plots are 10-year averages for the month of July. The original data were obtained as 10-minute averages every hour.

circumstances the data reveal unexpectedly large wind direction changes with height above the surface. Inspection of the data shows that this feature can be given a phenomenological description by making an analogy to the thermal wind effect.

An attempt is being made to model the diurnal cycle in the wind structure in order to demonstrate numerically the effect which a diurnal change in the thermal wind may have on the planetary boundary layer (PBL). The model is based on the boundary layer equations with the usual approximations and closure through K-theory. In this time dependent, "horizontally homogeneous" PBL with a thermal wind and steady geostrophic wind, the diffusivity K_m is related to a mixing length λ through $K_m = b \cdot \lambda(z, t) \cdot u_*(z, t)$, where b is a constant, u_* is the local friction velocity, and $\lambda = cz/\varphi$ defines a function φ. In a stationary surface boundary layer φ equals

$$\varphi_m = \frac{kz}{u_*} \frac{\partial|\overline{V}|}{z} .$$

For $z \to z_o$, it is assumed that $\varphi \to \varphi_m$ also in the non-stationary case, i.e. the von Karman constant $k = b \cdot c$. Furthermore it is assumed that the response of the PBL to time variations in the spatial boundary conditions can be described by

$$\frac{\partial u_*^2}{\partial t} = \frac{u_{*s}^2 - u_*^2}{T} \quad \text{and} \quad \frac{\partial \lambda}{\partial t} = \frac{\lambda_s - \lambda}{T} ,$$

where the "time constant" T is $T = a\lambda/u_*$, and a is a constant. The subscript "s" refers to solutions to the equations for the stationary cases, which are solved with φ as a specified function of height and the stability parameter $G/(fL)$. Here G is the geostrophic wind speed, f is the Coriolis parameter, and L is the surface value of the Monin-Obukhov stability length.

The problems encountered in the numerical treatment of the equations have not yet been fully solved, but preliminary results show agreement between model and observations.

Air - Sea Interaction I (Kattegat)

(N. E. Busch, L. Kristensen, and S. E. Larsen in co-operation with the Institute of Physical Oceanography, University of Copenhagen, and the Geophysical Institute of the University of Bergen)

During the first two weeks of May 1973, a 40 m tower weighing 2.5 tons was successfully erected in the Kattegat at the position 56° 36' N, 12° 05' E. The average water depth at that position is approximately 25 m and the distance to the nearest shore about 20 nautical miles. In the prevailing wind direction, the unobstructed fetch is 2 to 3 times longer. The tower was secured to the sea bottom by six guy wires and a similar number of anchors, each of which weighed 2 tons. The under-water part of the tower was instrumented with sensors for measurements of current, salinity, and temperature profiles. Above the sea surface the tower carried instruments for measurements of wind and temperature profiles. The data were collected in situ digitally on magnetic tape.

The plans were to keep the tower in operation for a period of 5 months during which additional shorter term experiments were to be carried out concerning turbulence in and above the water, optical properties of sea water, internal waves, and surface waves. However, in the night between the 10th and 11th of June while a 15-20 m/s storm was blowing, the tower was rammed by an unknown vessel. The tower was wrecked and sank to the bottom.

With kind assistance from the Danish Navy and the Danish Coast Lighting Authorities,[x)] the instruments as well as the tower were later recovered. Although the installations had suffered some damage, the direct economic loss turned out to be small. Far more important is the loss of 4 months of tower operation. Nevertheless, one month of data were obtained and are now being analysed. The plans for the future are to repeat the experiment in 1975 and to continue and to increase the activity over a period of 3 years. In order to make detailed turbulence measurements in and above the water feasible, the tower must be equipped with a fast, high-resolution telemetry system. Such a system is presently under consideration.

Air - Sea Interaction II (JONSWAP)

(N. E. Busch and S. E. Larsen)

The Second Joint North Sea Wave Project (JONSWAP 2) was carried out during the month of September 1973 west of the Isle of Sylt. Deutsches Hydrographisches Institut and Universität Hamburg were in charge of the co-ordination of the experiment, which received heavy support from the German Sonderforschungsbereich and from NATO.

The experimental objectives of JONSWAP 2 were threefold: to measure the spatial and temperal structure of the surface wave field with an array of surface instruments and with instrumented aircraft, to obtain remote-

x) Department under the Royal Danish Administration of Navigation and Hydrography

sensing data from aircraft in conjunction with this ground-truth data, and to measure interactions between the wave field and the atmospheric boundary layer. The first two of these objectives were largely attained, the last - and most difficult - only partially.

Risø's Meteorology Section was invited to participate in the last-mentioned attempts to obtain direct air - sea interaction data by means of detailed turbulence measurements in the lowest 10-15 m of the atmosphere over the sea. The measurements were to be made on one of two bottom-fast needles located 15 nautical miles off the coast of Sylt (Station 8-PISA).

In co-operation with DISA Electronics A/S and the Electronics Department, Risø, an instrument package was developed. It comprises (1) fast responding wind vanes equipped with three-component hot-wire probes, vertically aligned U-hot-wire probes, and a cold-wire for resistance

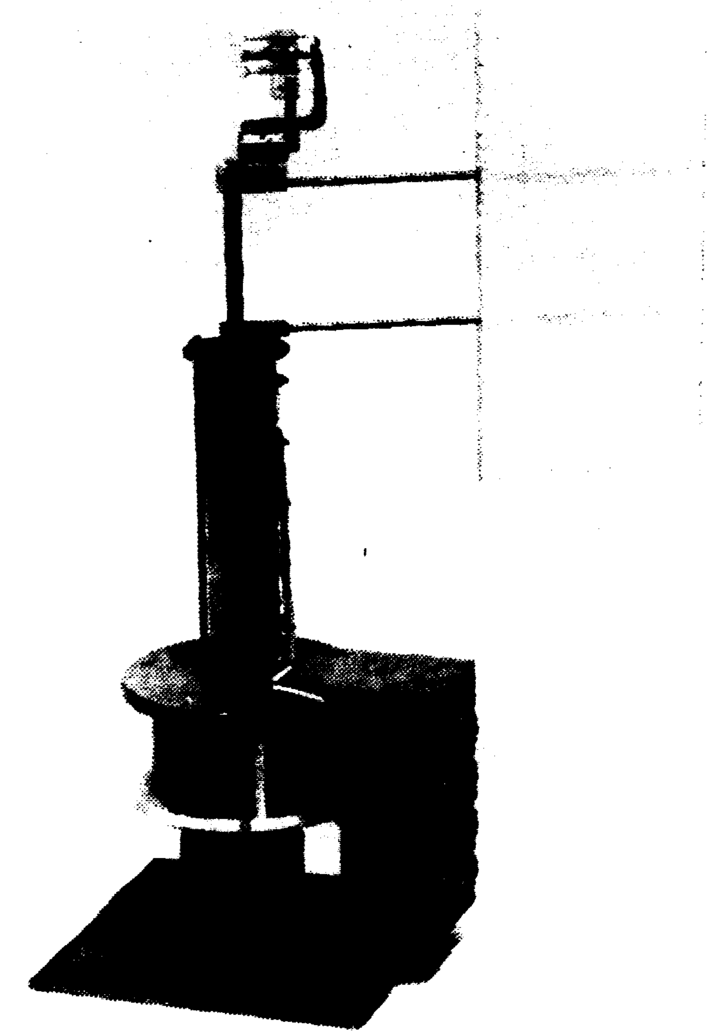

Fig. 18. Fast responding wind vane with hot-wires and cold-wire. The probes are arranged on top of the vane on a probe head (see fig. 19), which is easily unplugged and changed. The electric connection between the rotating and the stationary parts is provided by 10 mercury contacts. The vane position is measured by means of a precision potentiometer. The dimensions of the vane blade are 10, 20, and 0.7 cm.

thermometry, (2) Lyman-alpha humidiometers, and (3) two water-tight containers with anemometers, linearizers, temperature bridge, filters and amplifiers, power supplies, and the necessary logic circuits for remote telemetry control of the system. The system has proved itself highly reliable and easy to operate. The experience gained during the JONSWAP 2 experiment and later showed that a few minor changes in the instrumentation are desirable.

Owing to bad weather and numerous problems with the German telemetry system, the experiments at Station 8-PISA could not be carried out. The problems included late delivery, a series of debugging problems, short-circuits caused by electrical discharges during a thunderstorm, and intermittent malfunctioning of the PISA power supply. Nevertheless, the experience gained with the interaction instrumentation under rough North Sea conditions should prove invaluable for future experiments.

It is possible that a smaller, less ambitious trial experiment will be undertaken next year at Station 8-PISA. However, on account of the 1974 GARP Tropical Experiment (GATE) to which many participating groups are committed, it is probable that the next JONSWAP experiment will not take place until 1975.

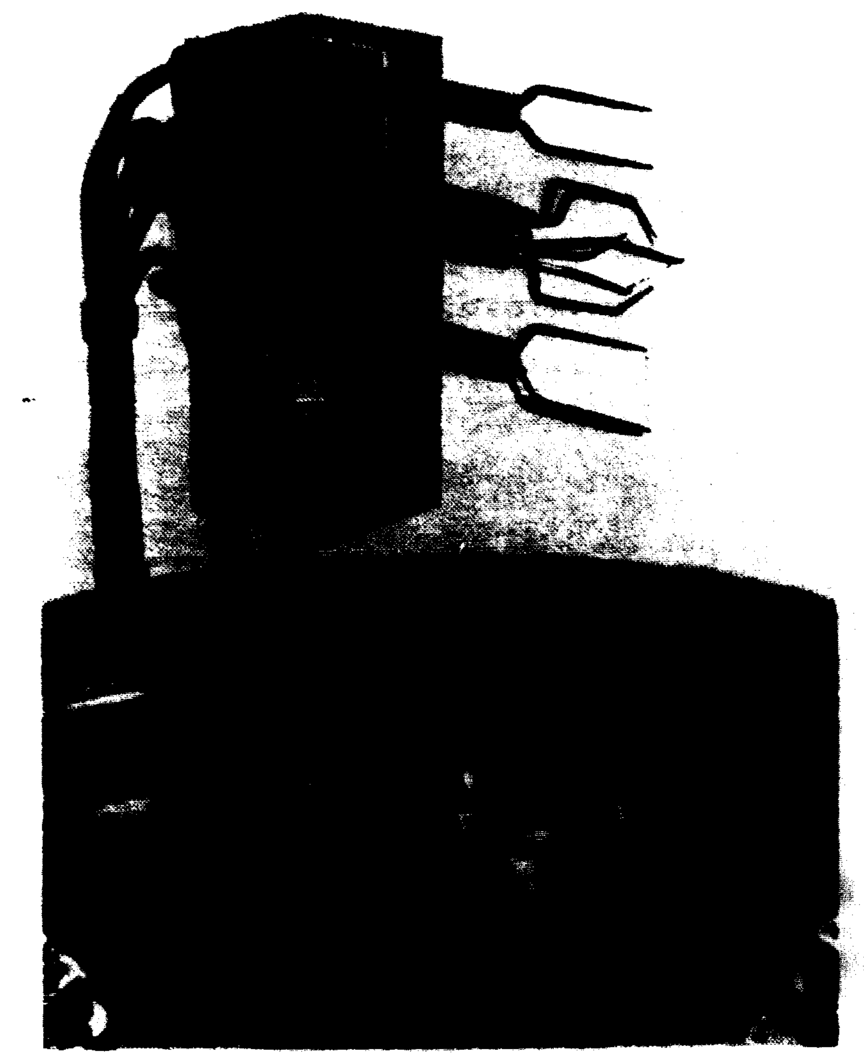

Fig. 19. Probe head with hot-wires and cold-wire (see also fig. 18). The top probe is a vertically alligned 5µ tungsten hot-wire with an active length of 1.25 mm (total length: 3.25 mm). The probe in the middle is a 3-dimensional hot-wire probe. The three wires have the same characteristics as the one above. The lowest probe is a V-shaped cold-wire for resistance thermometry. It is 6.25 mm long and has a thickness of 5µ.

Fine Structure Experiment

(N. E. Busch, N. O. Jensen, L. Kristensen, S. E. Larsen, C. H. Gibson (University of California, San Diego), and N. Boston (Naval Postgraduate Shcool, Monterey))

In November 1973 an experiment was conducted at Risø in which cold-wire thermometry and hot-wire anemometry were employed in conjunction with Lyman-alpha humidiometers and ultrasonic anemometers in order to investigate the shape of the spectra at relatively high frequencies (probably up to 1-2 kHz). Special emphasis was given to the measurements of fast temperature fluctuations. A variety of cold-wire probes were used (thickness: 0.25, 0.63, 1, and 5μ) with a number of fast AC- and DC-bridges. Measurements were made 2 and 60 m above terrain. The data were recorded as analogue signals on magnetic tape recorders and also digitally at a rate of 200 a second.

Kind assistance from the Computer Group at Risø made a prompt, preliminary analysis of some of the digital records possible. Unexpected differences in the temperature spectra obtained by means of different probes and bridges are being investigated. The differences are in most cases small but undoubtedly significant. Some strong-wind cases at 2 m height show marked 5/3 power laws in all spectra (velocity, temperature, and humidity). One apparently very stationary run at 60 m height shows a horizontal velocity spectrum with four decades of 5/3 power law. The data await more detailed analysis. A similar but more extensive joint experiment is in the planning stage for the summer of 1974.

Climatology in Greenland

(N. E. Busch, L. Kristensen, and J. Taagholt (Ionosphere Laboratory, Danish Meteorological Institute))

At the same time as a steadily increasing scientific, technical, and economic interest is taken in the exploration of artic regions, the funds for continuation of geophysical and meteorological research in Greenland are dwindling. Last year this fact prompted the design and installation of a relatively simple and inexpensive Unmanned Geophysical Observatory (UGO) at Nord in North Greenland. The UGO records air temperatures, pressure, wind speeds, and wind directions on an hourly basis. The data are recorded by means of a small transportable datalogger equipped with a magnetic tape recorder. This self-contained, battery-powered climatological station should be capable of $1\text{-}1\frac{1}{2}$ years of operation without maintenance if necessary. So far the data brought back by the sledge patrol "SIRIUS" (of the Royal Danish Air Force) give cause for optimism is spite of the severe climatic conditions under which the station operates.

This year a similar UGO was installed approximately 200 km west of Nord at the Jørgen Brønlund Fjord in Pearyland (82° 02' N, 31° 05' W). The first 2-3 months of data have been recovered. The quality of the measurements appears to be high.

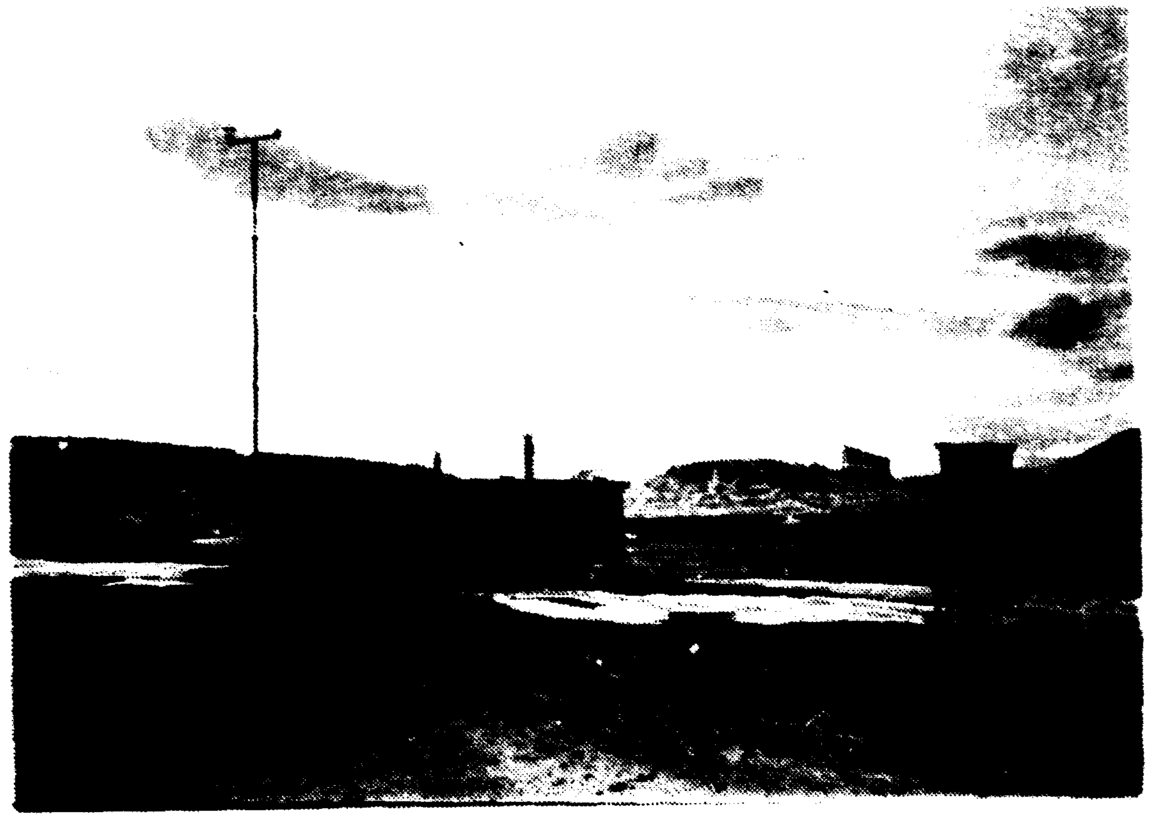

Fig. 20. View from the SE of the arctic station Kap Harald Moltke at Brønlund Fjord. Left the cup anemometer and the wind-direction sensor mounted on a 6 m steel pipe. Right the Stevenson screen with temperature sensors. Soil temperature is measured below the Stevenson screen. The barometer and the datalogger are installed in the building.

Spectral Analysis of Climatological Data

(L. Kristensen and E. L. Petersen)

The analysis of energy spectra for the horizontal mean wind components (hourly) was continued on the basis of the Risø record and data obtained elsewhere (e. g. Greenland). Analyses in terms of the total horizontal wind speed do not yield a realistic picture of the distribution of kinetic energy on mean flow and "eddies" nor do they yield physically relevant distributions of the energy on frequencies. Analyses of zonal and meridional energy spectra, however, revealed a number of interesting results. One of them is that for frequencies corresponding to periods shorter than 3-4 days but longer than 2-3 hours, the kinetic energy spectra for the zonal and the meridional components are almost identical, which indicates that the horizontal flow possesses certain statistical symmetry properties.

In spite of the fact that Coriolis forces as a consequence of their

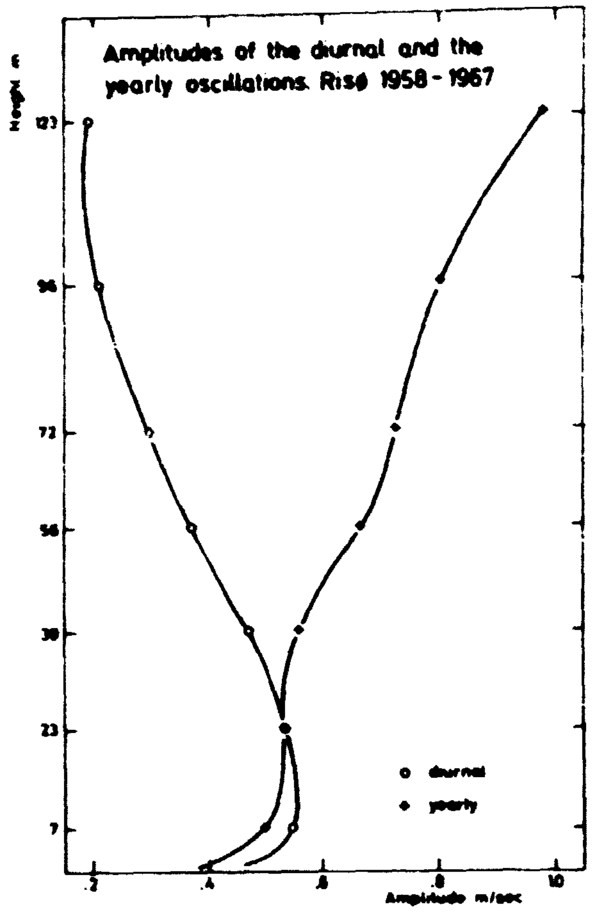

Fig. 21. Amplitudes of the diurnal and yearly variations in horizontal wind speeds. The amplitudes are estimated from Fourier decomposition of 10 years of hourly data from the height indicated.

fictitious nature neither create nor destroy energy, it is found that they are of importance for the distribution of energy on components as well as frequencies. Data from North Greenland and from Risø support the suggestion that the influence of Coriolis forces on the frequency distribution of kinetic energy close to the North Pole is markedly different from the influence exercised by these forces in the temperate zone. The records from Greenland are yet not sufficiently long to permit firmer or farther reaching conclusions, but the work will be continued.

Statistical Analysis of Extreme Wind Velocities

(O. Christensen)

The present Danish Building Code specifies design wind velocities without regard to the joint probability associated with the occurrence of extreme winds with a given wind direction. In many cases, however, a construction may be rather insensitive to even extremely high wind

provided the wind does not attack within specific and often relatively narrow wind direction sectors. Therefore an attempt is made towards a reformulation of the code in terms of the probability with which extreme winds occur within specified wind direction sectors. Wind data obtained from the 120 m Risø tower on an hourly basis through more than 15 years have been used in a preliminary study.

Applied Meteorology

(N. E. Busch, O. Christensen, N. O. Jensen, L. Kristensen, and S. E. Larsen)

This year as earlier, the Meteorology Section undertook a number of tasks of an applied nature. Among these were: Site evaluation and dispersion modelling, development and testing of meteorological instruments, air pollution studies, and evaluation of effects of wind loading on buildings and other structures.

With special reference to calculations of air pollution dispersal, the climatological record obtained at Risø during the years 1958 through 1967 was reanalysed. The data were grouped in 12 wind-direction sectors, 7 stability categories, and 5 wind-speed intervals. The frequency of recurrence within each group is given in tabular form and some results are presented graphically (Risø-M-Report No. 1666).

In support of a study undertaken by Dansk Kedelforening (The Danish Boiler Association) of air quality in the vicinity of a large power plant, a 40 m meteorology tower was erected at Stigsnæs in the southwestern part of Sealand. The tower is instrumented with wind speed sensors at three heights and with wind direction and temperature sensors at two heights. The data are compiled digitally on magnetic tape. The installation has been in routine operation since the beginning of July 1973.

Storkøbenhavns Luftforureningsudvalg (The Air Pollution Committee for Copenhagen) has implemented investigations of air pollution in Copenhagen. The means comprise a mobile monitoring station, which is moved to a new location every two weeks. The Meteorology Section has instrumented the van with wind-speed, wind-direction, and temperature sensors in conjunction with an atumatic datalogger. In order to supplement these measurements as well as those performed by the Danish Meteorological Institute along a 250 m tower in Copenhagen (Gladsaxe Radio and Television Tower), another two meteorological stations were put into operation, one in Central Copenhagen (Margretheholmen), the other on the western outskirts (Herstedvester). For a while the latter suffered from considerable electric noise problems as it is installed in an antenna tower belonging to a complex of the most powerful radio transmitters in Denmark. At both stations wind speeds and directions are measured at a height of approximately 40 m. Temperatures are measured 2 m and 40 m above terrain. The data acquisition is automatic (digital magnetic tape).

The development of sturdy, light-weight cup assemblies for rotating cup anemometers has been brought to an end. The cup assemblies are made of carbon-reinforced plastic (carbon fibres in a matrix of Araldite). They have been tested in a wind tunnel, have undergone accelerated ageing, and have been tested for cold resistance. The assemblies easily withstood wind speeds of 80 m/s. They did not show significant signs of deterioration after 991 hours of alternating arc lamp exposure and water spraying (estimated equivalent to approximately 3 years in the atmosphere). Submergence of the cups in liquid N_2 (-196°C) apparently did not affect the mechanical properties of the material seriously. The density of the cup material is approximately 1.3 g/cm^3, and its tensile strength approximately 14 kp/mm^2 (for comparison the corresponding numbers for St37-steel are 7.8 g/cm^3 and 37 kp/mm^2). This work was performed in collaboration with W. Batsberg Pedersen and H. Lilholt of the Chemistry Department and Metallurgy Department respectively.

5. LIQUID-N_2 AND -He PLANT

The production of liquid N_2 and He amounted to 140000 and 17000 litres respectively. Out of these 7200 litres of liquid He was delivered to laboratories in Copenhagen and Århus.

6. EDUCATIONAL ACTIVITIES AND PUBLICATIONS

Lectures

J. Als-Nielsen, Kernefysik (50 lectures in nuclear physics). Technical University of Denmark.

J. Als-Nielsen, Kernefysiske modeller ("Models in Nuclear Physics", 2 lectures given in a course for Danish high school teachers). University of Copenhagen (October 1973).

B. Buras, Nuclear Methods in Solid State Physics (lecture series) University of Copenhagen.

B. Buras, Inelastic Scattering of Neutrons by Phonons (6 lectures and subsequent neutron scattering experiments). University of Copenhagen and Risø.

B. Buras, Neutron Diffraction Studies of Samples at High Pressures. University of Copenhagen (November 1973).

N.E. Busch, Vejr, Klima og Luftforurening ("Weather, Climate, and Air Pollution"). Selskabet for Naturlærens Udbredelse, University of Copenhagen (March 1973).

N.E. Busch, Nonuniformity of Atmospheric Boundary Layers. Pennsulvania State University, U.S.A. (April 1973).

K. Caneiro and M. Nielsen, Neutron Scattering in Solid and Liquid H_2. NATO Advanced Study Institute on Anharmonic Lattices, Structural Transitions and Melting, Ustaoset Høyfjellshotel, Norway (April 1973).

C.T. Chang, Some Aspects of the Pellet Refuelling Problem. Institute of Plasma Physics, KTH, Stockholm, Sweden (June 1973).

C.T. Chang, Problems concerning Pellet Refuelling of a Fusion Reactor - Theoretical Aspects. Institute of Plasma Physics, KTH, Stockholm, Sweden (November 1973).

C.J. Christensen, A Search for Fission Isomer Formation with Thermal Neutrons. Argonne National Laboratory, U.S.A. (August 1973).

O.W. Dietrich, Neutronfysik (5 lectures in neutron scattering). Institute of Physics, University of Århus.

N. O. Jensen (3 doble lectures). Technical University of Denmark (October 1973):
1) Meteorologi og Aerodynamik i Relation til Luftforurening. ("Meteorology and Aeorodynamics in Relation to Air Pollution").
2) Atmosfæriske Spredningsmekanismer og Modeller. ("Atmospherical Scattering Mechanisms and Models").
3) Røgfanemodeller, Anvendelser og Begrænsninger. ("Plume Dispersion Models, Applications and Limitations").

V. O. Jensen, Plasmafysik (50 lectures in Plasma Physics). Technical University of Denmark.

V. O. Jensen, Plasma Fysik og Kontrolleret Termonuclear Fusion. (" Plasma Physics and Controlled Termonuclear Fusion"). (2 lectures). Faculty of Natural Sciences, University Center of Roskilde (April and November 1973).

S. E. Larsen, Dispersal of Aerosols in the Atmosphere. Meeting on Air-Borne Injection and Ventilation. Danish Pathology Society, Copenhagen (March 1973).

S. E. Larsen, Risø-Analysen af Camp-Century Serien. ("The Risø Analysis of the Camp-Century Series"). University of Copenhagen (April 1973).

P. Michelsen, Nonlinear Coupling between Electromagnetic and Ion Acoustic Waves:
1) Yale University, New Haven, U. S. A. (February 1973).
2) Danish Space Research Institute (April 1973).

M. Nielsen, Phonons in Solid and Liquid Hydrogen studied by Inelastic Neutron Scattering:
1) Argonne National Laboratories, Illinois (December 1972).
2) Duke University, Durham, North Carolina (January 1973).
3) Brookhaven National Laboratory, New York (July 1973).
4) Oak Ridge National Laboratory, Tennessee (August 1973).
5) University of California, Los Angeles (September 1973).

N. W. Nielsen, Kansas Eksperimentet. En Eksperimentel Verifikation af Monin-Obukhov Similaritetshypotesen. ("The Kansas Experiment. An Experimental Verification of the Monin-Obukhov Simuiarity Hypothesis"). Institute of Theoretical Meteorology, University of Copenhagen (March 1973).

H. L. Pécseli (3 lectures). Chalmers Tekniska Högskola, Göteborg, Sweden (September 1973):
1) Experimental Investigations of a Q-Machine Plasma.
2) Turbulence Measurements in a Q-Machine.
3) Investigation of Plasma Oscillations in terms of van Kampen Modes.

E. L. Petersen, Beskrivelse og Modellering af Instationære og Horizontalt Inhomogene Atmosfæriske Grænselag. ("Description and Modelling of Non-Stationary and Horizontally-Inhomogeneous Atmospheric Boundary Layers"). Technical University of Denmark (March 1973).

S. Shapiro, Structural Phase Transition. University of Århus (November 1973).

J. Wenzel, Structure of Amorphous Ice. A. E. C. Summer School on Neutron Diffraction, MIT, Cambridge, Mass. (August 1973).

F. Øster, Problems concerning Pellet Refuelling of a Fusion Reactor - Experimental Aspects. Institute of Plasma Physics, KTH, Stockholm, Sweden (November 1973).

Publications

P. Bak and P. -A. Lindgård, Magnetic Properties of Nd-Group V Compounds. J. Phys. C 6 (1973) 3774-3784.

R. J. Birgeneau, L. W. Rupp, Jr., H. J. Guggenheim, P. -A. Lindgård, and D. L. Huber, Critical Electron-paramagnetic-resonance Spin Dynamics in $NiCl_2$. Phys. Rev. Lett. 30 (1973) 1252-1255.

B. Buras and J. K. Kjems, Moving Crystal Slow-Neutron Wavelength Analyser. Nucl. Instrum. Methods 106 (1973) 461-464.

B. Buras, J. Staun Olsen, A. Lindegaard Andersen, L. Gerward, and B. Selsmark, Energy-Dispersive Spectroscopic Method Applied to X-ray Diffraction in Crystals. Physical Laboratory II, H. C. Ørsted Institute, University of Copenhagen Monograp No. 73-12 (1973) 38 pp. (Published also as Report No. 4 of Laboratory of Applied Physics III, Technical University of Denmark).

B. Buras, J. Staun Olsen, A. Lindegaard Andersen, L. Gerward, and B. Selsmark, Evidence of Escape Peaks Caused by a Si(Li) Detector in Energy-Dispersive Diffraction Spectra. Physical Laboratory II, H. C. Ørsted Institute, University of Copenhagen Monograph No. 73-23 (1973) 4 pp. (Published also as Report No. 5 of Laboratory of Applied Physics III, Technical University of Denmark and accepted for publication in the Journal of Applied Crystallography).

N. E. Busch, The Surface Boundary Layer. Boundary-Layer Meteorol. 4 (1973) 213-240.

N. E. Busch, B. R. Bean, Y. Furuhama, G. A. McBean, and J. Strohbehn, Turbulence Spectra at Scales Smaller than 1 meter. Boundary-Layer Meteorol. 5 (1973) 211-217.

N. E. Busch, On the Mechanics of Atmospheric Turbulence. In: Workshop on Micrometeorology. Edited by D. A. Hangen (American Meteorological Society, Boston, 1973) 1-65.

N. E. Busch, Vejr, Klima og Luftforurening. In: Forureningens Hvem Hvad Hvor. (Politikens Forlag, København, 1973) 99-136.

N. E. Busch, Weather and Climate Factors in Industrial Site Evaluation with Respect to Air Pollution. In: Environmental Engineering. Edited by G. Lindner and K. Nyberg (D. Reidel, Dordrechs, 1973) 81-94.

K. Carneiro, M. Nielsen, and J. P. McTague, Collective Excitations in Liquid Hydrogen observed by Coherent Neutron Scattering. Phys. Rev. Lett. 30 (1973) 481-485.

C. T. Chang, On Poor Separation in a Magnetically Driven Shock Tube. Plasma Phys. 15 (1973) 1265-1267.

G. B. Christoffersen and L. P. Prahm, Observations of Two-Stream Ion Wave Instability. Phys. Fluids 16 (1973) 708-710.

O. Danielsen, Magnetism of NaCl Type Uranium Compounds. Risø-M-Report No. 1658 (1973) 20 pp.

J. A. Dutton, The Global Thermodynamics of Atmospheric Motion. Tellus 25 (1973) 89-110.

J. A. Dutton, Recent Perspectives on Turbulence in the Free Atmosphere. In: Turbulence in the Free Atmosphere. By N. K. Vinnichenko, N. Z. Pinus, S. M. Shmeter and G. N. Shur. (Consultants Bureau, New York, 1973) 1-30.

M. T. Evans, E. Warming, M. T. Hutchings, and M. W. Stringfellow, Optic Spin-Waves in Magnetite near the Verwey Transition. Solid State Commun. 12 (1973) 795-798.

H. C. S. Hsuan and V. O. Jensen, Study of Ion Acoustic Wave Damping through Green's Functions. Phys. Fluids 16 (1973) 1776-1778.

N. O. Jensen, Occurrence of Stability Classes, Wind Speeds, and Wind Directions as observed at Risø. Risø-M-Report No. 1666 (1973) 37 pp.

V. O. Jensen and P. I. Petersen, On Collisionless Damping of Ion Acoustic Waves. Phys. Lett. 45 A (1973) 293-294.

L. W. Jørgensen and H. L. Pécseli, Calculations of Propagation of Density Perturbations in Collisionless Plasmas. Risø Report No. 299 (1973) 45 pp.

L. Kristensen and J. Taagholt, Unmanned Geophysical Observatory at Nord in North Greenland. Danish Meteorological Institute (1973) 80 pp.

A. R. Mackintosh, Mechanisms of Magnetic Anisotropy in Rare Earth Metals. Magnetism and Magnetic Materials - 1972, American Institute of Physics (1973) 1256-1258.

K. A. McEwen, G. J. Cock, L. W. Roeland, and A. R. Mackintosh, High-Field Magnetization of Light Rare-Earth Metals. Phys. Rev. Lett. 30 (1973) 287-290.

P. Michelsen and H. L. Pécseli, Propagation of Density Perturbations in a Collisionless Q-Machine Plasma. Phys. Fluids 16 (1973) 221-225.

A. H. Millhouse and K. A. McEwen, Neutron Diffraction Study of Single Crystal Europium in an Applied Magnetic Field. Solid State Commun. 13 (1973) 339-345.

M. Nielsen, Phonons in Solid Hydrogen and Deuterium Studied by Inelastic Coherent Neutron Scattering. Phys. Rev. B 7 (1973) 1626-1635.

H. L. Pécseli and P. I. Petersen, Electron Heating in a Single-ended Q-Machine. Risø Report No. 290 (1973) 17 pp.

E. L. Petersen and P. A. Taylor, Some Comparisons between observed Wind Profiles at Risø and Theoretical Predictions for Flow over Inhomogeneous Terrain. Quart. J. Roy. Meteorol. Soc. 99 (1973) 329-336.

P. I. Petersen, Kontrolleret Fusion. Fysik Tidsskrift 6 (1972) 145-160.

H. Sørensen and H. H. Andersen, Stopping Power of Al, Cu, Ag, Au, Pb, and U for 5-18-MeV Protons and Deuterons. Phys. Rev. B 8 (1973) 1854-1863.

F. Øster, The Possibility of Pellet Injection and Preliminary Experimental Results. Course on the Stationary and Quasi-Stationary Toroidal Reactors (EURATOM Luxembourg) EUR 4999 (1973) 373-384.

Conference Contributions

J. Als-Nielsen and L. M. Holmes, Critical Neutron Scattering from an Ising, Dipolar Ferromagnet, $LiTbF_4$. Danish Solid State Society, General Meeting, Munkebjerg, 31 May - 2 June 1973.

O. K. Andersen and O. Jepsen, Electronic Structure ar ' Phase Transition in Yb. The Physics of the Rare Earth Metals, Helsingør, 29 August - 1 September 1973.

P. Bak and P. -A. Lindgård, Theory of Magnetic Properties of Nd-Pnictides. International Conference on Magnetism, Moscow, 22-28 August 1973.

P. Bak and P. -A. Lindgård, Theory of Magnetic Properties of Nd-Pnictides. Danish Solid State Society, General Meeting, Munkebjerg, 31 May - 2 June 1973.

H. Bjerrum Møller, Neutron Scattering from Superfluid Helium. Nordic Solid State Physics Conference, Gausdal, Norway, 4-9 January 1973.

H. Bjerrum Møller, Neutron Scattering. Inaugural Meeting of the Danish Physical Society at H. C. Ørsted Institute, Copenhagen, 15 December 1973.

B. Buras, J. Staun Olsen, A. Lindegaard Andersen, L. Gerward, and B. Selsmark, X-ray Diffraction Using an Energy Dispersive Spectrometer. Danish Solid State Society, General Meeting, Munkebjerg, 31 May - 2 June 1973.

B. Buras, W. Kofoed, and B. Lebech, Neutron Diffraction Studies of Samples under High Pressure. Danish Solid State Society, General Meeting, Munkebjerg, 31 May - 2 June 1973.

B. Buras, K Carneiro, S. E. Nielsen, E. Præstgaard, and S. Steenstrup, Neutron Cooling by Bragg Reflection from Moving Crystals. Danish Solid State Society, General Meeting, Munkebjerg, 31 May - 2 June 1973.

N. E. Busch, Wind Structure in the Planetary Boundary Layer. Its Relation to the Diurnal Cycle and Nonuniformity of Surface Temperature. Second IUTAM-IUGG Symposium on Turbulent Diffusion in Environmental Pollution, Charlottesville, Virginia, 8-14 April 1973.

N. E. Busch, On the Role of Empirical/Statistical Modelling of Air Quality. Proc. 4th Meeting of the Expert Panel on Air Pollution Modelling, VIII 1-4, NATO/CCMS, Oberursel, BRD, 28-30 May 1973.

N. E. Busch, N. O. Jensen, and S. E. Larsen, Wind Structure in the Planetary Boundary Layer. Symposium on the Atmospheric Boundary Layer, Verband Deutscher Meteorologischer Gesellschaften, Mainz, 10-12 October 1973.

K. Carneiro, Collective Excitations in Liquid Hydrogen Observed by Coherent Neutron Scattering. Danish Solid State Society, General Meeting, Munkebjerg, 31 May - 2 June 1973.

K. Carneiro, M. Nielsen, and J. P. McTague, Collective Excitations in Liquid Hydrogen Observed by Coherent Neutron Scattering. Société de Chimie Physique, 24th Annual Meeting, Orsay, France, July 1973.

C. T. Chang, On Separation Distance in a Magnetically Driven Shock Tube. Eleventh International Conference on Phenomena in Ionized Gases, Prague, Czechoslovakia, 10-14 September 1973. In: Book on Contributed Papers, p. 367.

C. T. Chang, Remarks Concerning Experimental Simulation of the Pellet Refuelling. Sixth European Conference on Controlled Fusion and Plasma Physics, Moscow, 30 July - 4 August 1973. In: Contributed Papers 1, 349-352.

O. Danielsen, Temperature Dependence of the Magneto-Crystalline Anisotropy in Hexogonal Crystals. Danish Solid State Society, General Meeting, Munkebjerg, 31 May - 2 June 1973.

O. W. Dietrich, Inelastic Neutron Scattering as a Probe in Molecular Dynamics. Nordic Meeting on Molecular Physics, Fredensborg, 25-26 May 1973.

O. W. Dietrich, Review and Analysis of Experimental Data on Critical Scattering (3 lectures). Conference on Critical Phenomena, Wladyslawowo (Cetniewo), Poland, September 1973.

O. W. Dietrich and J. Als-Nielsen, A Comparison of the NMR, the Specific Heat, and the Neutron Scattering Methods for Studies of Magnetic Excitations in EUO and EUS. Danish Solid State Society, General Meeting, Munkebjerg, 31 May - 2 June 1973.

F. Y. Hansen and K. Carneiro, Neutron Scattering from Amorphous Selenium. Danish Solid State Society, General Meeting, Munkebjerg, 31 May - 2 June 1973.

L.M. Holmes, H.J. Guggenheim, and J. Als-Nielsen, Neutron Study of Crystal-Field Excitations in $LiTbF_4$. International Conference on Magnetism, Moscow, 22-28 August 1973.

J. Gylden Houmann, Phonons, Magnon-Phonon Interactions, and Magnetic Anisotropy. The Physics of the Rare Earth Metals, Helsingør, 29 August - 1 September 1973.

H.C.S. Hsuan, V.O. Jensen, and P. Michelsen, On the Initial Value Problem of an Ion Acoustic Wave in a Weakly Unstable Plasma. 15th APS Plasma Physics Meeting, Philadelphia, October-November 1973. In: Bull. Am. Phys. Soc. 18 (1973) 1290.

H.C.S. Hsuan, V.O. Jensen, and P.I. Petersen, Ion Acoustic Waves Studied Through Green's Functions. Conference on Waves and Instabilities in Plasmas, Innsbruck, 2-7 April 1973.

J. Jensen, J. Gylden Houmann, H. Bjerrum Møller, and A.R. Mackintosh, Anisotropic Exchange Interaction between the Magnetic Ions in Terbium. Nordic Solid State Physics Conference, Gausdal, Norway, 4-9 January 1973.

J. Jensen and J. Gylden Houmann, Anisotropic Exchange Interaction between the Magnetic Ions in Terbium. Danish Solid State Society, General Meeting, Munkebjerg, 31 May - 2 June 1973.

J. Jensen and J. Gylden Houmann, Anisotropic Exchange Interaction between the Magnetic Ions in Terbium. International Conference on Magnetism, Moscow, 22-28 August 1973.

J. Jensen, Magnetoelastic Effects and Elastic Constants. The Physics of the Rare Earth Metals, Helsingør, 29 August - 1 September 1973.

O. Jepsen, Phase Transitions in Ytterbium. Energy Bands and Fermi Surface of the hcp Phase. Danish Solid State Society, General Meeting, Munkebjerg, 31 May - 2 June 1973.

S.E. Larsen, N.E. Busch, and N.W. Nielsen, Characteristic Scales in the Atmospheric Surface Layer. Symposium on the Atmospheric Boundary Layer, Verband Deutscher Meteorologischer Gesellschaften, Mainz, 10-12 October 1973.

B. Lebech, B.D. Rainford, and F.A. Wedgwood, The Magnetic Form Factor of Praseodymium. International Conference on Magnetism, Moscow, 22-28 August 1973.

B. Lebech and B.D. Rainford, Applied Magnetic Field Effects in Double-hexagonal Close-Packed Neodymium. International Conference on Magnetism, Moscow, 22-28 August 1973.

B. Lebech and B.D. Rainford, Effects of Applied Magnetic Fields on the Magnetic Structure of Double-hexagonal Close-Packed Neodymium. Danish Solid State Society, Topical Meeting on Crystallography, Technical University of Denmark, 14 November 1973.

P.-A. Lindgård, J. Als-Nielsen, R.J. Birgeneau, and H.J. Guggenheim (Bell Lab. U.S.A.), Spin Wave Dispersion and Magnetization in $NiCl_2$. International Conference on Magnetism, Moscow, 22-28 August 1973.

P.-A. Lindgård and S.H. Liu, Exchange Interaction in the Heavy Rare Earth Metals Calculated from Energy Bands. Danish Solid State Society, General Meeting, Munkebjerg, 31 May - 2 June 1973.

P.-A. Lindgård and S.H. Liu, Exchange Interaction in the Heavy Rare Earth Metals Calculated from Energy Bands. International Conference on Magnetism, Moscow, 22-28 August 1973.

P.-A. Lindgård and S.H. Liu, Exchange Interaction in the Heavy Rare Earth Metals Calculated from Energy Bands. The Physics of the Rare Earth Metals, Helsingør, 29 August - 1 September 1973.

A.R. Mackintosh, K.A. McEwen, G.J. Cock and L.N. Roeland, Magnetism of Light Rare Earths in Enormous Fields. Danish Solid State Society, General Meeting, Munkebjerg, 31 May - 2 June 1973.

A.R. Mackintosh, Tungsten Bronzes Revisited. Danish Solid State Society, General Meeting, Munkebjerg, 31 May - 2 June 1973.

A.R. Mackintosh, Summary (Experimental). The Physics of the Rare Earth Metals, Helsingør, 29 August - 1 September 1973.

J.P. McTague, M. Nielsen, and K. Carneiro, Collective Excitations in Liquid Hydrogen Observed by Coherent Neutron Scattering. American Physical Society Meeting, San Diego, March 1973.

M. Nielsen and H.G. Smith (Oak Ridge National Laboratory), Lattice and Molecular Vibrations in Iodine. Symposium on Molecular Vibrations and Spectroscopy, Ohio State University, 15 June 1973.

H.L. Pécseli, Step-like Density Perturbations in a Collisionless Q-Machine Plasma. Conference on Waves and Instabilities in Plasmas, Innsbruck, 2-7 April 1973.

O. Rathmann, Long-Range Order in β-Brass by Neutron Diffraction. Danish Solid State Society, General Meeting, Munkebjerg, 31 May - 2 June 1973.

J. Wenzel and C. Linderstrøm-Lang, Structure of Amorphous Ice. Danish Solid State Society, General Meeting, Munkebjerg, 31 May - 2 June 1973.

J. Wenzel and C. Linderstrøm-Lang, Structure of Amorphous Ice by Neutron Scattering. International Conference on Water and Aqueous Solutions, Marburg, July 1973.

F. Øster, Grupperapport om Plasmafysikarbejdet ved AEK. ("Work in Plasma Physics at Risø"). Plasma og Gassutladningssymposiet, Otta, Norway, February 1973.

Degrees, Students, etc.

During the period the following members of the staff acquired the following degrees:

Erik Lundtang Petersen	lic. techn.

The following postgraduate students carried out research at the Physics Department towards the degree of lic. techn. (or Ph.D.):

Per Bak	(Solid-State Physics)
Kim Carneiro	(Solid-State Physics)
Oluf Danielsen	(Solid-State Physics)
Niels Otto Jensen	(Meteorology)
Leif Wagner Jørgensen	(Plasma Physics)
Hans Pécseli	(Plasma Physics)
Peter I. Petersen	(Plasma Physics)
Ole Rathmann	(Solid-State Physics)
Jack Wenzel	(Solid-State Physics)

The following students from Danish universities completed or are working on M.Sc. thesis projects at the department:

Peter Aarosiin Hansen	(Solid-State Physics)
Niels Woetmann Nielsen	(Meteorology)

During January and August 1973 students from the Universities of Århus and Copenhagen took part in laboratory courses organized by staff members. The following courses were offered:

1) Neutron Scattering (K. Carneiro and E. Warming)

2) Plasma Physics (H. Pécseli, P.I. Petersen, and P. Michelsen)

Four foreign students sponsored by the IAESTE carried out practical work at the department as part of their general training.

7. STAFF OF THE PHYSICS DEPARTMENT

Hans Bjerrum Møller (head of department)

Office Staff

Alis Frellsen
Gerda Stauning
Alice Thomsen
Hélène Shapiro (temporary assistant)

1. Solid-State Physics (Neutron Physics)

Scientific Staff

Jens Als-Nielsen
Ole Krogh-Andersen (consultant, Technical University of Denmark)
Per Bak (Ph.D. student)
Bronislaw Buras (also at the H.C. Ørsted Institute)
Kim Carneiro (Ph. D. student)
Maurice Chapellier (consultant, H.C. Ørsted Institute)
Rodney M.J. Cotterill (consultant, Technical University of Denmark)
Oluf Danielsen (Ph.D. student) (until 15 September 1973)
Ove W. Dietrich
Jens Gylden Houmann
Lewis Holmes (also at the Technical University of Denmark) (until 15 April 1973)
Jens Jensen
Ove Jepsen
Kiril Krejov (IAEA stipendiate, until 28 June 1973)

Jørgen K. Kjems (at Brookhaven National Laboratory)
Jens Klæstrup Kristensen (Ph. D. student, also at the Technical University of Denmark)
Bente Lebech
Per-Anker Lindgård
Allan R. Mackintosh
Keith A. McEwen (also at the H. C. Ørsted Institute) (until 1 March 1973)
Hans Bjerrum Møller
Mourits Nielsen
Brian M. Powell (guest scientist from Chalk River Nuclear Laboratories (until 15 May 1973))
Hans-Georg Purwins (guest scientist from Université de Genève)
Ole Rathmann (Ph. D. student)
Stephen Shapiro (guest scientist from Brookhaven National Laboratory)
Petr Viščor (until 31 March 1973)
Elisabeth Warming
Jack Wenzel (Ph. D. student from the University of Chicago)

Technical Staff

Poul E. Bredahl
Bjarne Breiting
Svend Broeng (until 31 March 1973)
Kaj Christensen
Arent Hansen
Bent Heiden
John Z. Jensen
Louis G. Jensen
Steen Jørgensen
Werner Kofoed
Jens Linderholm
Jørgen Munck
Allan Thuesen
Knud Møllenbach (temporary assistant)

2. Plasma Physics

Scientific Staff

Che Tyan Chang
Nicola D'Angelo (consultant, Danish Space Research Institute

Vagn O. Jensen
Leif Wagner Jørgensen (Ph. D. student)
Poul Michelsen
Hans Pécseli (Ph. D. student)
Peter I. Petersen (Ph. D. student)
Alfred H. Sillesen
Hans Sørensen
Flemming Øster

Technical Staff

Bendix Bordrup (until 14 January 1973)
Bengt Hurup Hansen
Mogens Nielsen
Arne Nordskov
John Petersen
Børge Reher
Hans Skovgård
Jane Doyle (temporary assistant)

3. Nuclear Physics

Scientific Staff

Verner Andersen
Carl Jørgen Christensen
David Shackleton (also at the Niels Bohr Institute)

Technical Staff

Poul Andersen
Finn Hansen

4. Meteorology

Scientific Staff

Niels E. Busch
Ole Christensen (also at ISVA, the Technical University of Denmark)
Niels Otto Jensen (Ph. D. student)
Leif Kristensen
Søren E. Larsen
Niels Woetmann Nielsen (M. Sc. student)
Erik Lundtang Petersen (Ph. D. student until April 1973, presently at Pennsylvania State University)

Technical Staff

Jørgen Christensen
Gunner Dalsgård
Morten Frederiksen
Gunner Jensen
Knud Sørensen

5. Liquid-N_2 and -He Plant

Technical Staff

John Z. Jensen
Poul E. Bredahl
Bent Ferdinandsen (part-time assistant from the Service Department)

Visiting Scientists (one to three month visits)

B. Bonnevier, Kungliga Tekniska Högskolan, Stockholm	**(Plasma Physics)**
N. E. J. Boston, Naval Postgraduate School, Monterey	**(Meteorology)**
R. A. Cowley, University of Edinburgh	**(Solid-State Physics)**
C. H. Gibson, University of California	**(Meteorology)**
K. Hennig, Dubna	**(Solid-State Physics)**
J. Herbst, H. C. Ørsted Institute and Cornell University	**(Solid-State Physics)**
H. C. S. Hsuan, University of Iowa	**(Plasma Physics)**
J. P. McTague, University of California, Los Angeles	**(Solid-State Physics)**
E. W. Peterson, Oregon State University	**(Meteorology)**
T. Riste, IFA, Kjeller	**(Solid-State Physics)**
D. Sherrington, Imperial College, London	**(Solid-State Physics)**